Calculation of Electron Affinities of Polycyclic Aromatic Hydrocarbons and Solvation Energies of Their Radical Anion. Leon D. Betowski, Mark Enlow, Lee Riddick, and Donald H. Aue J…

ARTICLE *in* THE JOURNAL OF PHYSICAL CHEMISTRY A · JANUARY 2006

Impact Factor: 2.69

1 AUTHOR:

Betowski Don

United States Environmental Protection Age…

79 PUBLICATIONS **459** CITATIONS

SEE PROFILE

Calculation of Electron Affinities of Polycyclic Aromatic Hydrocarbons and Solvation Energies of Their Radical Anion

Leon D. Betowski,*,† Mark Enlow,†,# Lee Riddick,† and Donald H. Aue*,‡

U.S. Environmental Protection Agency, National Exposure Research Laboratory, Environmental Sciences Division, P.O. Box 93478, Las Vegas, Nevada 89193-3478, and Department of Chemistry and Biochemistry, University of California, Santa Barbara, California 93106

Received: September 5, 2006; In Final Form: September 12, 2006

Electron affinities (EAs) and free energies for electron attachment ($\Delta G°_{a,298K}$) have been directly calculated for 45 polynuclear aromatic hydrocarbons (PAHs) and related molecules by a variety of theoretical methods, with standard regression errors of about 0.07 eV (mean unsigned error = 0.05 eV) at the B3LYP/6-31+G(d,p) level and larger errors with HF or MP2 methods or using Koopmans' Theorem. Comparison of gas-phase free energies with solution-phase reduction potentials provides a measure of solvation energy differences between the radical anion and neutral PAH. A simple Born-charging model approximates the solvation effects on the radical anions, leading to a good correlation with experimental solvation energy differences. This is used to estimate unknown or questionable EAs from reduction potentials. Two independent methods are used to predict $\Delta G°_{a,298K}$ values: (1) based upon DFT methods, or (2) based upon reduction potentials and the Born model. They suggest reassignments or a resolution of conflicting experimental EAs for nearly one-half (17 of 38) of the PAH molecules for which experimental EAs have been reported. For the antiaromatic molecules, 1,3,5-tri-*tert*-butylpentalene and the dithia-substituted cyclobutadiene **1**, the reduction potentials lead to estimated EAs close to those expected from DFT calculations and provide a basis for the prediction of the EAs and reduction potentials of pentalene and cyclobutadiene. The Born model has been used to relate the electrostatic solvation energies of PAH and hydrocarbon radical anions, and spherical halide anions, alkali metal cations, and ammonium ions to effective ionic radii from DFT electron-density envelopes. The Born model used for PAHs has been successfully extended here to quantitatively explain the solvation energy of the C_{60} radical anion.

Introduction

Polynuclear aromatic hydrocarbons (PAHs) have been of great importance in the history of organic chemistry[1] and the early application of quantum mechanical calculations to large molecules in chemistry.[2] Their carcinogenicity[3] and prevalence in the environment from coal, petroleum, and combustion sources[4] have made them the subject of regulation by the U. S. Environmental Protection Agency (EPA).[5] Neutral and cationic forms of PAHs have been proposed to be a source of the diffuse interstellar emission bands.[6] Anionic PAHs may then play a role in the evolution of interstellar clouds and have been observed in experiments designed to measure their spectra.[7] Recent papers also focus on other important aspects of PAHs.[8−11] Analytical chemistry and toxicological studies on PAHs have implicated them as comprising one of the largest classes of environmental carcinogens.[12,13] Analysis for PAHs is now routine, but improved methods would be desirable, and recent attempts at natural attenuation[14] have led to renewed interest in methods for the analysis of PAHs in different soil types. Because PAHs often occur in complex matrixes, improved methods for more specific detection in the presence of other hydrocarbons and molecules would be useful. Structure-specific chemical ionization mass spectrometric methods based upon differential gas-phase basicities (GBs) have been proposed to help solve this problem with the aid of calculated GBs.[15,16] Negative-ion chemical ionization mass spectrometry is also a method that leads to enhanced sensitivity toward many PAHs.[17,18] Prediction of these sensitivities and the possible existence of anionic PAHs in interstellar space depends on knowledge of their electron affinities (EAs). In a related paper, we have shown that the combined use of experimental and calculated EAs can, in fact, be very useful in understanding negative-ion mass spectral sensitivities.[17b] In recent work, EAs have been calculated for some PAHs.[19] In this paper, we explore the efficacy of modern quantum mechanical methods for the calculation of EAs of a wide variety of 45 PAHs and related molecules, including all PAHs for which EAs are known experimentally.

Electron affinities are an important basic molecular property. Experimental EAs are known for many, but hardly all, important PAH molecules. Experimental determinations of electron affinities[19c,20] of PAHs come from electron-capture detection,[21] electron swarm,[22] equilibrium,[23] and bracketing[24] methods, collisional activation mass spectrometry,[25] electron transmission spectroscopy,[26] and laser photodetachment photoelectron spectroscopy.[27] We have previously found that gas-phase basicities of PAHs can be effectively calculated using semiempirical (AM1), Hartree−Fock (HF), second-order Møller−Plesset perturbation theory (MP2), and density functional (DFT) methods with standard errors in regressions with experimental

* To whom correspondence should be addressed. E-mail: aue@chem.ucsb.edu (D.H.A.) or betowski.don@epamail.epa.gov (L.D.B.).
† U.S. Environmental Protection Agency.
‡ University of California, Santa Barbara.
# Present address: Applied Research Associates, Inc., P.O. Box 40128, Tyndall AFB, FL 32403.

10.1021/jp065785v CCC: $33.50
Published on Web 11/09/2006

values ranging from 2.12 down to 1.36 kcal mol^{-1}.[16] The accurate calculation of EAs is a more challenging problem theoretically. Unlike ionization potentials (IPs), where Koopmans' Theorem[28] methods lead to fortuitous cancellation of electron correlation and ion relaxation effects, there is no such cancellation in the calculation of EAs. Since the direct calculation of EAs from the difference in the energies of the neutral and anionic PAH involves odd-electron systems, spin contamination can become a problem in the calculation of the anion, and diffuse functions may also be needed. Another approach is the use of Green's Function or propagator methods.[29] Like the Koopmans' Theorem approximation, Green's Function methods calculate ionization potentials and electron affinities as properties of the wave function of the neutral species and do not require an additional calculation for the radical cation or anion.

Previous theoretical studies on the negative ions of PAHs[6c,19,30] have only recently included correlated methods with diffuse basis sets. Numerous recent theoretical investigations of neutral and cationic PAHs have focused on the prediction of infrared spectra.[6,31−34] Schaefer and co-workers have shown that DFT can be an accurate method for predicting the electron affinities of various molecules and some hydrocarbons.[19,35−38] We will explore the applicability of a variety of the theoretical methods discussed above to the calculation of EAs of a wide range of PAHs and related molecules and compare with experimentally known values.

Theoretical Methods

Several methods have been used for the calculation of electron affinities. Since available experimental electron affinities of PAHs are largely adiabatic, the most direct theoretical method comes from calculation of the energies of both the neutral and anionic forms of the PAH at their respective optimized geometries, the "ΔE" method. We have also used Koopmans' Theorem to calculate EAs from LUMO energies of the neutral PAHs or from HOMO energies of their anions. In addition, the outer-valence Green's Function (OVGF) method has been used.[29,39] All calculations were performed using the Gaussian 94, Gaussian 98, and Gaussian 03 program suites.[40]

Complete geometry optimizations for the neutral and anionic forms of all molecules were first carried out by the Hartree−Fock (HF) method[41] with a 6-311G(d,p) basis set (HF/6-311G(d,p)) followed by frequency calculations. All geometries were reoptimized using density functional methods using Becke's three-parameter exchange functional with the Lee, Yang, and Parr correlation functional at the B3LYP/6-311G(d,p) level[42] and frequency calculations carried out in order to verify that the stationary points thus obtained were true minima and to determine thermodynamic parameters for the determination of reaction energetics. The 6-311G(d,p) basis set was used in these calculations because diffuse functions sometimes result in linear dependencies that interfere with self-consistent field (SCF) convergence in DFT methods; however, single-point B3LYP/6-31+G(d,p), B3LYP/6-311+G(2df,2pd), B3LYP/cc-pVDZ, B3LYP/aug-cc-pVDZ, B3LYP/cc-pVTZ, and B3LYP/aug-cc-pVTZ calculations at the B3LYP/6-311G(d,p) geometries were carried out to account for the effect of diffuse functions on reaction energetics with no SCF convergence problems. All of these DFT single-point calculations were carried out with the scf=tight option, which gives energies that can differ by as much as 0.25 kcal mol^{-1} from the default option. For 1,3-butadiene, cyclobutadiene, and pentalene and their anions, B3LYP/6-31+G(d,p) geometries and frequencies were calculated with no significant change in reaction energies, zero-point energy, or entropy from the B3LYP/6-311G(d,p) data. For 1,3-butadiene and cyclobutadiene, Møller−Plesset many-body perturbation theory at second order (MP2) up to fourth order (MP4 with single, double, triple, and quadruple electronic excitations, MP4SDTQ)[43] and the coupled-cluster method with noniterative triples (CCSD(T))[44] were employed. For all molecules, MP2 calculations were performed. Among basis sets used for MP2 calculations, the 6-31+G(d,p) basis has been shown to be an effective small basis set for energies of hydrocarbons[45,46] and was used for hydrocarbons and their radical anions up to 12 carbons. For hydrocarbons and their radical anions up to 24 carbons, MP2/6-31G(d) calculations were used. The larger Dunning correlation-consistent polarized valence triple-ζ basis with diffuse augmentation functions (aug-cc-pVTZ)[47] was used for the four-carbon molecules and ions. Calculations at the CCSD(T)/cc-pVTZ//MP2/6-31+G(d,p) level using MP2 geometries have been found to give accurate energies for hydrocarbons and carbocations, even for heats of formation based upon hydrogenolysis energies, where fortuitous error cancellation is minimized.[48] EAs at effectively the CCSD(T)/aug-cc-pVTZ//MP2/6-31+G(d,p) level were estimated from CCSD(T)/6-31+G(d,p), MP4/cc-pVTZ, and MP2/aug-cc-pVTZ levels assuming G2-like additivity of basis-set effects.[48]

For the open-shell radical anions, all calculations were done with spin-unrestricted methods, where spin contamination from quartet and higher spin states is a potential problem. Indeed, the UHF and UMP2 calculations showed large $<S^2>$ operator expectation values from 0.8229 to 2.2797 at UHF/6-311G(d,p), 0.7706 to 2.2969 at UMP2/6-31G(d), and 0.7711 to 1.1614 at UMP2/6-31+G(d,p). Remarkably smaller values were found with the UB3LYP method, with values (from 0.7523 to 0.7709) close to the expected 0.75 value for a pure doublet spin state. Calculations at the ROB3LYP/6-31+G(d,p) level for the anions (scf=tight) eliminate the contributions from higher spin states and give energies only 0.4−0.9 kcal mol^{-1} higher in energy than UB3LYP/6-31+G(d,p) energies, except for pentalene and coronene, which give energies 1.7 and 4.5 kcal mol^{-1} higher, and picene, which gives a different electronic symmetry, ^{2}B. The use of spin annihilation by Schlegel's projection method,[49] as implemented with PMP2 calculations in the Gaussian program, usually led to some improvement in spin contamination, and resulting PUHF and PUMP2 energies were used for calculation of EAs.

In the cases of benzo[*c*]phenanthrene (C_2), 1,1-diphenylethylene (C_2), cyclooctatetraene (D_{2d}), styrene (C_1), trans-stilbene (C_2 at the HF level, but C_{2h} at the DFT level), and biphenyl (D_2), the minimum-energy geometries for the neutral species were found to be nonplanar, as were the radical anions for benzo[*c*]phenanthrene (C_2), 1,1-diphenylethylene (C_2), picene (C_2), 1,3,5-triphenylene (C_2), and biphenyl (D_2). Other geometries are 1,3,5-trimethylpentalene (C_1, but near C_s with the symmetry plane of the rings), 1,3,5-trimethylpentalene anion (C_s, with the symmetry plane perpendicular to the rings), 1,3,5-tri-*tert*-butylpentalene and its anion (C_s with the symmetry plane of the rings), **1** and **2** and their anions (C_{2h}), **3** and its anion (C_2), anthracene−anthracene anion π complex (C_i) (B3LYP/3-21G frequency calcd, NImag = 0), end-to-end complex, and 9,9′-σ-bound complex (C_i) (B3LYP/3-21G frequency calcd, NImag = 1). The geometry of the C_{60} anion has been problematic, giving the C_i geometry as the minimum (NImag = 0), which lies only 0.01−0.03 kcal mol^{-1} lower in energy than the D_{3d} geometry. Details of geometries, molecular symmetries, ionic electronic states, and electronic energies are tabulated in the Supporting Information. The symmetries of benzene, triph-

enylene, and coronene were lowered slightly when computing the energies of the anions at the neutral geometries to avoid partial occupancy of degenerate LUMOs and attendant computational problems. Thermochemical data were calculated with zero-point energy corrections from scaled B3LYP/6-311G(d,p) frequencies using a scaling factor of 0.99 for DFT zero-point energies from linear regressions with experimentally known zero-point energies of organic molecules.[45,50] A scaling factor of 0.96 for DFT frequencies for the thermal and entropy terms was derived from linear regressions on experimental frequencies of organic molecules and PAHs.[7bd,45,50]

The calculations were performed either at the National Environmental Scientific Computing Center (NESC2) or locally on SGI Octane, Origin, Indigo2, or Dell Precision 390n workstations.

Results and Discussion

Experimental EA Data. A series of 45 PAHs and related molecules was chosen for calculation in this paper. These included 38 PAHs whose experimental EAs were available. The structures and names of many of these compounds are shown in Chart 1. Table 1 contains a summary of EA determinations for these molecules by various experimental methods.[20−27] The "EAs" from electron-transfer equilibrium methods (CID, Brack, IMRE, Kine in Table 1) are more properly regarded as free energies of electron attachment ($\Delta G°_{a,298K}$), while electron affinities are defined as adiabatic energies of electron attachment, $-\Delta E°_{a,0K}$. The electron swarm (ES) and electron-capture detection (ECD) methods can both give equilibrium constants for attachment of thermal electrons and energies that may also be regarded as free energies of electron attachment. With accurately scaled B3LYP/6-311G(d,p) frequencies, thermodynamic terms may be calculated as appropriate for each experimental method, as shown in Table 2.

Measurements of equilibrium constants at a particular temperature (IMRE) give free energies at that temperature, which are converted to enthalpies and a common scale of free energies at room temperature, $\Delta G°_{a,298K}$, in Table 2 using DFT-calculated entropies for electron transfer. The entropies for electron attachment are small, ranging from about 2 to 3 cal mol^{-1} K^{-1} for these PAHs. At the time that the experimental free energies were reported, accurate entropies for electron attachment to PAHs were not known, but such experimental data can be reanalyzed at this time. The adiabatic EA for the primary standard, sulfur dioxide, has been revised upward from 1.10 to 1.107 eV.[27i] The entropy for electron attachment for sulfur dioxide is calculated here from DFT frequency calculations to be 2.11 cal mol^{-1} K^{-1}, or 2.05 cal mol^{-1} K^{-1} from experimental frequencies.[23c] Thus, the revised $-\Delta G°_a$ value for sulfur dioxide is 1.13 eV at 298 K, 1.14 eV at 423 K, and 1.16 eV at 584 K, which leads to some small upward revisions in reported experimental free energies at these temperatures reflected in Table 1 for molecules determined by equilibrium methods. In Table 2, these experimental free energy data are converted to room temperature with DFT-calculated thermochemical terms, assuming that $\Delta H°_a$ is constant over the temperature range considered.

For temperature-dependent equilibrium measurements (TDEq), the experimental results are given as enthalpies for electron attachment, $\Delta H°_{a,298K}$, and can be converted to $\Delta G°_{a,298K}$ from entropies of electron attachment. These experiments on azulene, anthracene, and other aromatic molecules give entropies for electron attachment when related to the absolute entropy for sulfur dioxide.[23c−e] These experimental entropies differ from the DFT-calculated entropies, often by somewhat more than the expected experimental errors of about 2 cal mol^{-1} K^{-1}.[23c] Thus, the experimental and calculated entropies for electron attachment for azulene are 4.5 and 2.6 cal mol^{-1} K^{-1} and for anthracene

CHART 1: Structures of PAHs and Related Hydrocarbons

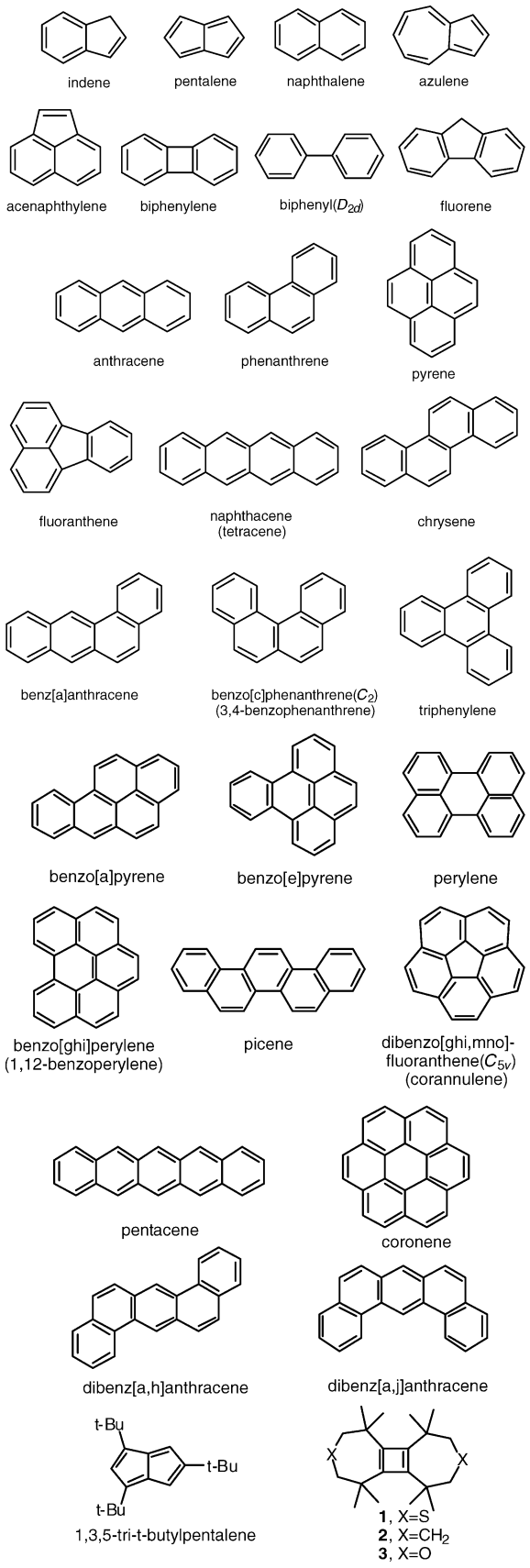

TABLE 1: Experimental "Electron Affinities" (EAs)

hydrocarbon	EA values (eV)[a]	methods[b]	refs
acenaphthylene	0.8, 0.41?	Est, ECD	21f
anthracene	0.53, 0.58, 0.61, 0.66, 0.48, 0.57, 0.556, 0.42, 0.56	LPES, IMRE(343 K), TDEq, ECD, ECD, ECD, ECD, CID	27c, 23c,f, 23e, 21i, 21f, 21c, 21b, 21a, 25a,b
azulene	0.79, 0.79, 0.70, 0.69, 0.70, 0.52, 0.656, >0.46	LPES, IMRE(423 K), TDEq, Kine(500 K), ECD, ECD, ECD, ES	27e, 23c−e, 23c, 23a, 21h, 21f, 21b, 22
benz[*a*]anthracene	0.70, 0.63, 0.46, 0.39?	ECD, ECD, ECD, CID	21i, 21b, 21a, 25a,b
benzo[*c*]phenanthrene	0.4, 0.54, 0.545, 0.33	Avg, ECD, ECD, ECD	21i, 21b, 21a
benzo[*a*]pyrene	0.79, 0.83, 0.68	IMRE(420 K), ECD, ECD	23f, 21i, 21a,b
benzo[*e*]pyrene	0.49, 0.534	ECD, ECD	21i, 21b
benzo[ghi]perylene	0.7, 0.42?	Est, CID	25a,b
biphenyl	−0.1, 0.15?, 0.13?	Est, ECD, ECD	21f, 21i,j
biphenylene	0.2, 0.89?	Est, CID	51, 25a,b
chrysene	0.42, 0.397, 0.33	ECD, ECD, ECD	21i, 21b, 21a
corannulene	0.8, 0.50?	Est, CID	25a
coronene	0.47, 0.54	LPES, CID	27h, 25a
dibenz[a,h]anthracene	0.68, 0.595	ECD, ECD	21i, 21b
dibenz[a,j]anthracene	0.6, 0.69, 0.591	Avg, ECD, ECD	21i, 21b
1,1-diphenylethylene	0.2, 0.40?	Est, ECD	21i,j
fluoranthene	0.7, 0.63?, 0.63?	Est, ECD, CID	21d, 25a,b
fluorene	−0.1, 0.28?	Est, ECD	21f
indene	−0.4, 0.17?	Est, ECD	21f
1-methylanthracene	0.55	CID	25b
1-methylnaphthalene	−0.2, 0.16?	Est, ECD	21f
2-methylnaphthalene	−0.2, 0.14?	Est, ECD	21f
naphthalene	−0.19, −0.20, −0.2, 0.15, 0.14, 0.148, 0.14	ETS, LPES est, Est, ECD, ECD, ECD, ECD	26a,b, 27f,g, 23c,e−g, 21i, 21g, 21b, 21f
naphthacene (tetracene)	1.04, 0.88	IMRE(458 K), ECD	23f, 21c
phenanthrene	0.1, 0.31?, 0.27, 0.307, 0.20, 0.31?	Est, ECD, ECD, ECD, ECD, CID	21i, 21f, 21b, 21a, 25a,b
pentacene	1.35	IMRE(589 K)	23f
perylene	0.97, 0.98, 0.35?	LPES, IMRE(425 K), CID	27d, 23f, 25a,b
picene	0.542	ECD	21b
pyrene	0.56, 0.591, 0.50, 0.39, 0.59	ECD, ECD, ECD, ECD, CID	21i, 21b, 21c, 21a, 25a,b
triphenylene	0.29, 0.285, 0.14	ECD, ECD, ECD	21i, 21b, 21a
benzocyclobutadiene	0.32	Brack(500 K)	24
cyclooctatetraene	0.65, 0.55, 0.577, 0.58	LPES, Kine(298 K), ECD, CID	27b, 23b, 21e, 25c
styrene	−0.1, 0.15?	Est, ECD	21i,j
trans-stilbene	0.35, 0.38	ECD, ECD	21i,j, 21f
diphenylacetylene	0.32	ECD	21f
benzene	−1.12, −1.13, −1.2	ETS, ETS, Est	26b, 26a, 21i
1,3-butadiene	−0.68	ETS	26a
C_{60}	2.689, 1.62?	LPES, CID	63, 25a
C_{70}	2.676	LPES	63

[a] Experimental electron affinities from different methods correspond to different thermodynamic quantities. Most methods give free energies of electron attachment ($\Delta G°_{a,298K}$), and exceptions are listed below for appropriate methods. Questionable experimental data based upon the analysis in this work are so indicated; see text. Preferred values are listed first and used in Table 2 and the following tables. For phenanthrene and fluoranthene, the somewhat doubtful experimental data are used in subsequent tables. They are similar to the, probably preferable, values estimated from reduction potentials in Table 2 and calculations in Tables 5 and 7. [b] Avg, approximate average of ECD values; Brack, bracketing reactions ($\Delta G°_{a,298K}$); ECD, electron-capture detector ($\Delta G°_{a,298K}$); CID, kinetic method by collisionally induced dissociation; ES, electron swarm ($\Delta G°_{a,298K}$); ETS, electron transmission spectroscopy ($\Delta E°_{a,0K}$); Est, estimated from half-wave reduction potential and correlation of solvation energy with ionic size (see text), from EA data of substituted naphthalenes for naphthalene, and from the best value for naphthalene for the methylnaphthalenes (see text); IMRE, ion−molecule reaction equilibrium ($\Delta G°_a$, measured at temperatures listed and corrected with DFT entropies and with new EA for SO_2; see text); Kine, from forward and reverse rate constants ($\Delta G°_{a,298K}$); LPES, laser photodetachment photoelectron spectroscopy ($\Delta E°_{a,0K}$); TDEq, temperature-dependent equilibrium ion−molecule reaction, $\Delta H°_{a,298K}$, corrected with new EA for SO_2; see text.

are −1.1 and 2.6 cal mol^{-1} K^{-1}, respectively. Since DFT calculations reproduce experimental vibrational frequencies quite well,[7] we expect that the theoretically estimated entropies will be more accurate than the experimental ones. We have, therefore, given preference to experimental free energy data and used the theoretical entropies to calculate enthalpies for electron attachment in Table 2. Experimental free energies have also been converted to $\Delta E°_{a,0K}$ and "electronic energies", $\Delta E°_{a,e}$, with DFT-calculated thermal and zero-point energy terms in Table 2. These energies, derived from experimental data, are used in Tables 3 and 4 for convenience of comparison with theoretically calculated energies. All thermodynamic calculations use the stationary electron convention and neglect the spin multiplicity of the electron.[20]

Laser photodetachment photoelectron spectroscopy (LPES) directly measures adiabatic EAs, $\Delta E°_{a,0K}$, provided that geom-

TABLE 2: Solution Reduction Potentials, Experimental Electron-Attachment Free Energies, and Solvent Effects[a]

			Experimental EA Data								
hydrocarbon	$-E_{1/2}$ vs Hg[b]	$-E_{1/2}$ vs SCE[b]	EA_{expt}[c]	$-\Delta E°_{a,e}$	$-\Delta E°_{a,0K}$	$-\Delta H°_{a,298K}$	$-\Delta G°_{a,298K}$	$-\Delta G°_{a,pred}$[d]	error in y vs Hg[e]	$-\Delta\Delta G°_{sol} - E_{1/2}$ pred vs Hg[f]	r[g]
1,3-butadiene	2.16	2.66	−0.68[h]	−0.87	−0.68	−0.71	−0.64	−0.59	−0.04	−2.69	3.00
cyclobutadiene	1.6	2.30	−0.08[i]	−0.30	−0.15	−0.18	−0.08	−0.13	0.05	−2.69	2.87
1	2.0	2.5	0.3[j]	0.21	0.30	0.31	0.3	0.26		−1.91	4.59
benzene	2.86	3.42	−1.12[h]	−1.39	−1.12	−1.17	−1.04	−1.19	0.15	−2.39	3.17
pentalene	0.4	0.9	1.4[j]	1.25	1.38	1.37	1.4	1.38		−2.41	3.36
1,3,5-tri-*t*-Bupentalene	0.95	1.45	1.3[j]	1.17	1.30	1.29	1.3	1.33		−1.96	4.67
styrene	1.96	2.65	−0.1[j]	−0.27	−0.11	−0.12	−0.1	−0.14		−2.35	3.45
cyclooctatetraene	1.12	1.62	0.65[h]	0.58	0.65	0.65	0.66	0.71	−0.05	−2.43	3.46
indene	2.25	2.77	−0.4[j]	−0.64	−0.43	−0.44	−0.4	−0.40		−2.36	3.50
azulene	1.10	1.60	0.79[h]	0.66	0.79	0.78	0.81	0.79	0.02	−2.30	3.59
naphthalene	1.99	2.51	−0.19[h]	−0.36	−0.19	−0.21	−0.16	−0.10	−0.06	−2.38	3.59
1-Menaphthalene	2.02	2.52	−0.2[h]	−0.37	−0.2	−0.21	−0.2	−0.07		−2.36	3.71
2-Menaphthalene	2.04	2.54	−0.2[h]	−0.37	−0.2	−0.21	−0.2	−0.09		−2.35	3.71
acenaphthylene	1.17	1.67	0.8[j]	0.65	0.78	0.77	0.8	0.78		−2.24	3.71
biphenylene	1.73	2.23	0.2[j]	0.05	0.19	0.18	0.2	0.22		−2.28	3.72
biphenyl	2.07	2.60	−0.1[j]	−0.31	−0.14	−0.16	−0.1	−0.08		−2.24	3.80
fluorene	2.12	2.62	−0.1[j]	−0.30	−0.13	−0.15	−0.1	−0.12		−2.19	3.84
anthracene	1.41	1.96	0.53[h]	0.29	0.53	0.50	0.60	0.61	−0.01	−2.20	3.89
phenanthrene	1.92	2.46	0.1[k]	−0.11	0.06	0.05	0.1	0.11		−2.19	3.90
diphenylacetylene	1.69	2.19	0.32	0.18	0.31	0.30	0.32	0.36	−0.04	−2.20	3.96
trans-stilbene	1.61	2.21	0.35	0.27	0.40	0.40	0.35	0.45	−0.10	−2.25	3.99
1,1-diphenylethylene	1.80	2.32	0.2[j]	0.05	0.20	0.19	0.2	0.26		−2.21	4.00
1-Meanthracene	1.42	1.92	0.55	0.39	0.53	0.52	0.55	0.65	−0.10	−2.24	4.02
fluoranthene	1.23	1.73	0.7[l]	0.55	0.68	0.67	0.7	0.84		−2.28	4.02
pyrene	1.53	2.10	0.56	0.39	0.54	0.52	0.56	0.54	0.02	−2.12	4.02
benz[*a*]anthracene	1.53	2.06	0.70	0.52	0.67	0.66	0.70	0.60	0.10	−1.98	4.17
benzo[*c*]phenanthrene	1.75	2.24	0.4	0.21	0.37	0.36	0.40	0.38	0.02	−2.06	4.19
chrysene	1.77	2.31	0.42	0.19	0.37	0.35	0.42	0.36	0.06	−2.02	4.19
naphthacene(tetracene)	1.14	1.64	1.04[m]	0.88	1.00	0.99	1.02	0.99	0.03	−2.05	4.18
triphenylene	1.91	2.46	0.29	−0.02	0.22	0.19	0.29	0.21	0.08	−2.01	4.17
corannulene	1.25	1.75	0.8[j]	0.47	0.66	0.63	0.8	0.84		−2.11	4.22
benzo[*a*]pyrene	1.31	1.99	0.79[m]	0.61	0.75	0.74	0.77	0.85	−0.08	−2.13	4.27
benzo[*e*]pyrene	1.58	2.17	0.49	0.29	0.46	0.44	0.49	0.58	−0.09	−2.14	4.27
perylene	1.17	1.67	0.97[h]	0.83	0.97	0.96	1.00	0.99	0.01	−2.04	4.26
benzo[ghi]perylene	1.49	1.99	0.7[j]	0.53	0.68	0.66	0.7	0.70		−2.02	4.37
pentacene	0.86	1.30	1.35[m]	1.19	1.30	1.30	1.32	1.35	−0.03	−2.03	4.43
picene	1.79	2.29	0.54	0.32	0.48	0.47	0.54	0.43	0.11	−1.88	4.45
dibenz[a,h]anthracene	1.55	2.05	0.68	0.49	0.65	0.64	0.68	0.66	0.02	−1.98	4.42
dibenz[a,j]anthracene	1.57	2.07	0.60	0.39	0.57	0.55	0.60	0.64	−0.04	−2.04	4.42
coronene	1.53	2.03	0.47[h]	0.20	0.47	0.44	0.57	0.69	−0.12	−2.11	4.45
C_{60}	−0.24	0.26	2.689[h]	2.50	2.69	2.65	2.78	2.69	0.09	−1.67	5.34
C_{70}	−0.24	0.26	2.676[h]	2.49	2.68	2.64	2.77	2.74	0.03	−1.68	5.77

[a] All values in electronvolts except ionic radii in angstroms. [b] Half-wave reduction potentials from refs 2, 21i, 51, 66, and 70, usually in DMF (0.1 M tetraalkylammonium salt). Values vs standard calomel electrode (SCE) from ref 21i (estimated from Hg electrode data using an avg. 0.5 V difference where quoted to 0.1 eV). Reduction potential for indene estimated from the measured difference in reduction peak potential from naphthalene in DMF, this work. The value for cyclobutadiene is estimated and fits the high-level-calculated EA, and that for pentalene is from the value for its tri-*tert*-butyl derivative; see text. [c] Electron affinities from Table 1, which are free energies for electron attachment, $\Delta G°_a$, except where noted otherwise. Experimental data are treated, as appropriate, to calculate other thermodynamic quantities using the B3LYP/6-311G(d,p) scaled frequencies; see text. [d] Predicted from the Hg reduction potentials in eq 1 and solvation effects predicted from the regression eq 4 with $1/r$; see text. [e] Residual error in $\Delta\Delta G_{sol}$ from linear regression, $y = mx + b$, with $\Delta\Delta G_{sol}$ as y and with $1/r$ as x in eq 4, excluding 16 points; see text. [f] Difference between solvation free energies of the neutral hydrocarbon and radical anion as in ref 21i with reference electrodevoltages of −4.21 V for Hg (and −4.71 V for SCE). [g] Ionic radius in angstroms calculated from the molecular volume of the hydrocarbon calculated in Gaussian from 0.001 e bohr^{-3} electron-density envelopes from B3LYP/6-31+G(d,p) calculations. [h] Electron-attachment energy from ETS for negative EAs (estimates for the methylnaphthalenes), or EAs from LPES experiments for positive EAs; both are treated as adiabatic EAs. [i] Calculated value of free energy from CCSD(T) data (see Table 4). [j] Experimental free energy suspect or missing. Estimated from reduction potential (vs Hg) and predicted solvent effect from regression with $1/r$. For pentalene, the value is estimated from the 1,3,5-tri-*t*-bupentalene value and DFT-calculated differences. [k] A value of 0.1 eV better fits the estimated value from reduction potential data, the DFT-calculated values in Table 5, and data in Table 7. [l] A value of 0.7 eV better fits the estimated value from reduction potential data, the DFT-calculated values in Table 5, and data in Table 7. [m] Free energy of electron-attachment at temperature given in Table 1. Original experimental data adjusted to 298 K using calculated entropies.

etry changes between the neutral and ionic species are small, as expected generally for PAHs. Electron transmission spectroscopy (ETS) attachment energies are often regarded as "vertical" negative EAs, close to adiabatic EAs, but this method actually detects resonance states in which the electron is unbound.[26a] Such data are treated here as adiabatic EAs and converted to the common free energy scale with DFT-calculated thermochemical data in Table 2. Where more than one value is reported in the literature, the first value listed in Table 1 is our preferred value. Where available, these were chosen from LPES or charge-transfer equilibrium free energy data. We have given preference to the LPES experiments. Such data are perhaps somewhat more reliable than free energy data and have the advantage that they give absolute values for the EAs. Furthermore, data from LPES and IMRE equilibrium free energies are generally in close agreement with one another after conversion of the LPES EAs to a common scale of free energies in Table 2. For example, this comparison for azulene gives derived

TABLE 3: Calculated and Experimental Electron Affinities for Representative PAHs from Koopmans' Theorem and ROVGF Methods[a]

	benzene	azulene	naphthalene	biphenylene
	$E_{LUMO}(M)$[b]			
HF/6-31G(d)	−4.08	−1.71	−2.82	−2.57
	[0.00]	2.37	1.26	1.51
HF/6-31+G(d,p)	−2.29	−1.15	−1.98	−1.86
	[0.00]	1.14	0.31	0.43
HF/6-311G(d,p)	−3.71	−1.47	−2.55	−2.30
	[0.00]	2.24	1.16	1.41
B3LYP/6-311G(d,p)	0.26	2.12	1.26	1.51
	[0.00]	1.86	1.00	1.25
	$E_{HOMO}(M^-)$[c]			
HF/6-31G(d)	−1.57	0.60	−0.58	−0.39
	[0.00]	2.17	0.99	1.18
HF/6-31+G(d,p)	−1.12	1.06	−0.18	0.01
	[0.00]	2.18	0.94	1.13
HF/6-311G(d,p)	−1.25	0.88	−0.31	−0.12
	[0.00]	2.13	0.94	1.13
HF/6-311G(d,p)[d]	−1.80	0.32	−0.92	−0.76
	[0.00]	2.12	0.88	1.04
B3LYP/6-311G(d,p)	−3.59	−1.19	−2.09	−1.51
	[0.00]	2.40	1.50	2.08
B3LYP/6-311G(d,p)[d]	−4.00	−1.50	−2.36	−1.90
	[0.00]	2.50	1.64	2.10
ROVGF/6-311G(d,p)	−2.61	−0.36	−1.55	−1.09
	[0.00]	2.25	1.06	1.52
experimental EA, $-\Delta E°_{0K}$	−1.12	0.79	−0.19	0.2(0.88)[e]
	[0.00]	1.91	0.93	1.2(1.92)[e]

[a] All values in electronvolts. Second-row entries are EAs relative to benzene. [b] Koopmans' Theorem EA from LUMO energy of neutral PAH at optimized geometries calculated at the same level. [c] Koopmans' Theorem EA from HOMO energy of radical anion of PAH at optimized geometries calculated at the same level. [d] Vertical Koopmans' Theorem EA from HOMO energy of radical cation at geometry of neutral PAH calculated at the same level. [e] Values in parentheses are suspect. The preferred values, estimated from solution reduction potentials, appear more accurate.

negative free energies of electron attachment of 0.80, 0.78, 0.73, and 0.67 eV for the LPES, IMRE, TDEq, and Kine data, respectively. Similarly, for anthracene, the free energies are 0.62, 0.58, and 0.64 eV for the LPES, IMRE, and TDEq data, respectively. For perylene, the LPES and IMRE data give negative free energies of 0.99 and 0.97 eV, respectively. For cyclooctatetraene, the agreement is less good; the LPES and Kine data give free energies of 0.66 and 0.55 eV, respectively.[23b,27b] The PES is not expected to show an adiabatic EA because of the large geometry change, but combining the experimental EA and an experimental estimate of the conformational energy correction gives an estimated adiabatic EA value of 0.65 eV.[27b] Whether this value or that from the equilibrium experiment is more accurate is not clear, but the LPES value will be shown later to be most consistent with theoretical estimates and solution data.

The close agreement between experimental free energies and LPES data suggests that the LPES method normally gives adiabatic values. We tested whether geometry changes between the neutral and ionic species are small, as required for adiabatic transitions, by comparing the HF/6-311G(d,p) energies of the radical anions for many PAH species at the neutral and optimized anion geometries. The differences were fairly constant for 20 PAHs, with the geometry relaxation energies ranging from 0.26 to 0.46 eV, except for biphenyl where a larger geometry change gives a 0.67 eV relaxation energy. Similar comparisons at the B3LYP/6-311G(d,p) level gave much smaller relaxation energies, ranging from 0.08 to 0.32 eV, with cyclobutadiene and biphenyl at 0.32 eV, styrene at 0.19 eV, and cyclooctatetraene at 1.07 eV for its large change to a planar anionic geometry. The DFT-calculated relaxation energies are judged the more reliable and are tabulated in the Supporting Information. Such calculations, at effectively the CCSD(T)/aug-cc-pVTZ level for butadiene, reduced the relaxation energy from 0.29 eV at the DFT level to only 0.15 eV. On the basis of these data and the upcoming agreement found between experimental data and theoretical calculations, we believe that differences between vertical and adiabatic EAs will usually be small and should hardly affect comparisons of trends in the EAs.

The ECD data from many determinations usually agree well with one another, even though the data sometimes come from treatments of the temperature-dependent response data using both the common-intercept[21b] and determined-intercept[21e,i] methods. The ECD measurements are similar to free energy measurements, usually within 0.1 eV, in accord with the presumption that this method measures free energies.

For naphthalene, however, there is a major inconsistency between ECD and ETS experiments, with the former indicating a positive EA and the latter a negative one. Careful attempts at equilibrium experiments indicate that the anion is not bound,[23c,e,f] and extrapolation of reliable equilibrium data for naphthalene derivatives[23e−g] is quantitatively consistent with the apparently adiabatic EA of −0.19 eV for naphthalene from ETS measurements.[26a,b] This analysis is confirmed by experimental LPES data for sequentially hydrated naphthalenes and naphthalene dimers, trimers, etc., where extrapolation to naphthalene leads to EAs of −0.20 and −0.18 eV, respectively.[27e,h] Further confirmation of this assignment for the EA of naphthalene is found in our estimate of the EA from the solution reduction potential, as discussed later.

Thus, the electron-capture data for naphthalene seem to be spurious.[23e,f] Such experiments do not directly identify the negative ions formed and might be ambiguous for other molecules, as well. Presumably, the ECD EAs are similarly flawed for the methylated naphthalenes, which should have values near −0.2 eV judging from the small effect of methyl substitution predicted theoretically and observed for 2-methylanthracene. These problems call into question the accuracy of other ECD data, especially for molecules with low EAs, biphenyl, 1,1-diphenylethylene, fluorene, indene, and styrene.[17b] Furthermore, there are several molecules for which the ranges of ECD values are as large as 0.1−0.2 eV or more.

In the case of perylene, there is a large disagreement between the low value from the collisionally induced dissociation method and the higher values from equilibrium and photodissociation data. For benz[*a*]anthracene, the CID value again appears anomalous compared with ECD data. It appears that the collisionally induced dissociation data are misleading, which calls into question the validity of other CID data.

It was hoped that calculational results and an analysis of reduction potential data in solution[2,51] would help resolve experimental problems such as those identified above. The experimental data which we regard as questionable for 17 molecules are designated in Table 1 with a question mark. New recommended values are given there as the first-listed EA based upon the analysis of experimental EAs, solution reduction potentials, and quantum calculations that follow.

In our initial analysis of experimental EA data in comparison with different theoretically calculated EAs, we immediately noticed that the EA of biphenylene, from a CID experiment, was the most anomalous. To test whether this might be the result of problems with the theory for biphenylene, perhaps related to its antiaromaticity, we studied other antiaromatic molecules,

TABLE 4: Calculated and Experimental Electronic Electron Affinities for Representative Hydrocarbons from the Δ*E* Method and Electronic Electron Affinities Relative to Benzene[a]

	1,3-buta-diene	cyclo-butadiene	benzene	pentalene	benzocyclo-butadiene	styrene	cycloocta-tetraene	azulene	naphtha-lene	biphenyl-ene
$-\Delta E°_{a,e}$[b]										
HF/6-31G(d)	−2.21	−1.80	−2.87	0.15	−1.35	−1.74	−0.96	−0.14	−1.73	−1.52
	0.66	1.07	[0.00]	3.02	1.52	1.13	1.91	2.73	1.14	1.35
HF/6-311G(d,p)	−1.91	−1.49	−2.54	0.37	−1.09	−1.47	−0.72	0.08	−1.47	−1.26
	0.63	1.05	[0.00]	2.91	1.45	1.07	1.82	2.62	1.07	1.28
HF/6-31G(d)[c]	−2.20	−1.84	−2.86	0.19	−1.36	−1.73	−0.95	−0.13	−1.72	−1.51
	0.66	1.02	[0.00]	3.05	1.50	1.13	1.91	2.73	1.14	1.35
PHF/6-31G(d)[c]	−1.95	−1.76	−2.58	0.79	−1.21	−1.18	−0.86	0.62	−1.44	−1.33
	0.63	0.82	[0.00]	3.37	1.37	1.40	1.72	3.20	1.14	1.25
MP2/6-31G(d)[c]	−2.21	−1.34	−2.90	−0.10	−1.02	−2.06	−0.41	−1.17	−1.60	−0.98
	0.69	1.56	[0.00]	2.80	1.88	0.84	2.49	1.73	1.30	1.92
PMP2/6-31G(d)[c]	−2.01	−1.31	−2.68	0.40	−0.89	−1.59	−0.36	−0.49	−1.38	−0.84
	0.67	1.37	[0.00]	3.08	1.79	1.09	2.32	2.19	1.30	1.84
HF/6-31+G(d,p)[d]	−1.57	−1.10	−2.24	0.73	−0.80	−1.25	−0.51	0.22	−1.28	−1.07
	0.67	1.14	[0.00]	2.97	1.44	0.99	1.73	2.46	0.96	1.17
PHF/6-31+G(d,p)[d]	−1.4	−1.03	−2.01	1.28	−0.66	−0.91	−0.43	0.79	−1.02	−0.89
	0.61	0.98	[0.00]	3.29	1.35	1.10	1.58	2.80	0.99	1.12
MP2/6-31+G(d,p)[d]	−1.24	−0.33	−1.97	0.60	−0.28	−1.15	0.21	−0.42	−0.92	−0.34
	0.73	1.64	[0.00]	2.57	1.69	0.82	2.18	1.55	1.05	1.63
PMP2/6-31+G(d,p)[d]	−1.11	−0.26	−1.79	1.06	−0.17	−0.87	0.26	0.09	−0.72	−0.21
	0.68	1.53	[0.00]	2.85	1.62	0.92	2.05	1.88	1.07	1.58
B3LYP/6-311G(d,p)	−1.00	−0.43	−1.68	1.09	0.00	−0.53	0.59	0.46	−0.42	0.00
	0.68	1.25	[0.00]	2.77	1.68	1.15	2.27	2.14	1.26	1.68
B3LYP/6-31+G(d,p)[e]	−0.59	0.02	−1.32	1.33	0.25	−0.25	0.81	0.65	−0.24	0.16
	0.73	1.34	[0.00]	2.65	1.57	1.07	2.13	1.97	1.08	1.48
B3LYP/	−0.58	0.00	−1.31	1.34	0.27	−0.20	0.85	0.69	−0.20	0.20
6-311+G(2df,2pd)[e]	0.73	1.31	[0.00]	2.65	1.58	1.11	2.16	2.00	1.11	1.51
B3LYP/aug-cc-pVDZ[e]	−0.53	0.08		1.38	0.31	−0.18		0.72	−0.17	
B3LYP/cc-pVTZ[e]	−0.87	−0.28	−1.56	1.18	0.09	−0.43	0.70	0.54	−0.35	0.06
B3LYP/aug-cc-pVTZ[e]	−0.55	0.01		1.35	0.27	−0.21	0.86	0.69	−0.20	
CCSD(T)/aug-cc-pVTZ[f]	−0.91	−0.30								
experimental $\Delta G°_{a,298K}$	−0.64	−0.1[h,i]	−1.04	1.4[h]	0.29	−0.1	0.66	0.81	−0.16	0.2(0.89)[j]
experimental $-\Delta E°_{a,e}$[g]	−0.87	−0.3[h,i]	−1.39	1.3[h]	0.13	−0.3	0.58	0.66	−0.36	0.1(0.74)[j]
	0.52	1.1[k]	[0.00]	2.7	1.52	1.12	1.97	2.05	1.03	1.4(2.13)[j]

[a] All values in electronvolts. Second-row entries are all electronic EAs relative to benzene. [b] Electronic EAs from difference in electronic energies of the hydrocarbon and its anion at geometries optimized at same level, except as noted. Exceptional geometries are found at the HF/6-31G(d) level for 1,3-butadiene anion (C_2) and at the HF/6-311G(d,p) level for 1,3-cyclobutadiene anion (C_2) and benzocyclobutadiene anion (C_s). [c] Geometries optimized at the B3LYP/6-311G(d,p) level. Spin annihilation by the projection method gives PUHF and PMP2 energies. [d] Geometries optimized at the MP2/6-31+G(d,p) level except for cyclobutadiene, benzene, and benzocyclobutene, which were optimized at the B3LYP/6-311G(d,p) level. Spin annihilation by the projection method gives PUHF and PMP2 energies. [e] Geometries optimized at B3LYP/6-311G(d,p) level. Single-point calculations done with scf=tight. [f] Estimated from EAs at the CCSD(T)/6-31+G(d,p), MP4/cc-pVTZ, and MP2/aug-cc-pVTZ levels assuming additivity of effects.The MP2 and MP4 (est) values for 1,3-butadiene and cyclobutadiene were −0.89 (MP2) −0.92 (MP4), and −0.20 (MP2) −0.30 (MP4) eV, respectively. The "vertical" EA calculated at the CCSD(T)/aug-cc-pVTZ level by additivity using the MP2 geometry of neutral butadiene was −1.06 eV. Geometries optimized at the MP2/6-31+G(d,p) level. [g] Experimental values corrected to electronic EA values by subtracting out ZPE, thermal, and entropy terms from B3LYP/6-31+G(d,p) frequencies, except for benzene, naphthalene, and 1,3-butadiene, where experimental appearance energies should contain no thermal or entropy term. [h] Experimental free energy suspect. Estimated from reduction potential (vs Hg) and solvent effect with regression with $1/r$. [i] The electron in the cyclobutadiene anion is expected to be unbound (ref 26a). [j] Value in parentheses suspect (preferred value estimated from solution reduction potential appears more accurate). [k] Difference between the experimental value for benzene and the CCSD(T) value for cyclobutadiene, which is judged more accurate than the estimated experimental value.

cyclobutadiene, pentalene, and cyclooctatetraene. The first two molecules in this set had no experimental EA values, but literature values for the reduction potentials for their derivatives, **1** and 1,3,5-tri-*tert*-butylpentalene, were found for comparison, as well as for biphenylene. If the gas-phase EAs could be estimated from the related solution reduction potentials, then we might be able to confirm whether the gas-phase EA for biphenylene has a value consistent with its solution reduction potential and to see how experimental data for the other antiaromatic molecules compared with theoretical EAs. As we shall see, it is the CID experiment on biphenylene that appears anomalous, rather than the theoretical result.

Table 2 contains two sets of experimental reduction potential data and a summary of the most reliable experimental gas-phase "EA" data selected from the various sources in Table 1. This EA data have been converted to a common scale of EAs, $\Delta E°_{a,0K}$, and $\Delta G°_{a,298K}$ values for the electron-attachment reaction using theoretical thermochemical parameters as described above. We will use the $\Delta G°_{a,298K}$ data set for most subsequent comparisons. The $\Delta G°_{a,298K}$ values for molecules whose experimental EAs are suspect, or not known, are reported to only one decimal accuracy and have been estimated by methods described below from theoretical calculations and experimental reduction potentials. The right-hand columns in Table 2 relate to the analysis of the reduction potential data and derived solvation energies in terms of ionic size.

Solution Reduction Potentials and Radical Anion Solvation. Correlations between EAs and half-wave reduction potentials ($E_{1/2}$)[2,21i,51] in solution would be useful in the analysis of questionable experimental EA data, provided that such correlations were quantitatively reliable. Such comparisons between gas-phase EAs and solution reduction potentials depend directly on the effect of solvation energies upon the electron-attachment process, as illustrated in the thermodynamic cycle in Scheme 1. In correlations of EA with $E_{1/2}$ for some sets of molecules, it has been observed, or presumed, that the slopes

SCHEME 1: Thermodynamic Cycle for the Analysis of Solution Effects on the Electron Attachment Reaction

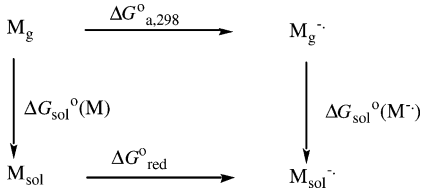

are nearly 1.0, indicating that the solvation energies are nearly constant within the set.[21i,k,23] This need not always be true,[52] and a more detailed analysis of the solvation energies might be warranted when slopes deviate from unity or when linear correlations are poor. As described in eqs 1 and 2, the differences in relative energies of electron attachment in the gas phase and solution are equal to the differences in the free energies of solvation of the neutral hydrocarbons and their radical anions, $\Delta\Delta G^\circ_{sol}$.[53]

$$\Delta\Delta G^\circ_{sol} = \Delta G^\circ_{sol}(M^{-\bullet}) - \Delta G^\circ_{sol}(M) \quad (1)$$

$$\Delta\Delta G^\circ_{sol} = \Delta G^\circ_{red} - \Delta G^\circ_{a,298K} = (E_{ref} - E_{1/2}) - \Delta G^\circ_{a,298K} \quad (2)$$

The solvation energies for neutral PAHs are not generally well-known, but some experimental data do exist for water and other solvents.[54] The free energies, enthalpies, and entropies of solvation for PAHs follow a pattern of hydrophobic solvation similar to that of other hydrocarbons in water, with relatively large, but nearly offsetting, enthalpy and entropy terms.[54] The free energies of many neutral molecules, including some PAHs, have been modeled with quantum mechanical and various semiempirical methods that include cavitation, van der Waals (dispersion), and electrostatic terms.[55] For PAHs, unlike alkanes, the free energies become slightly more negative, by a few kcal mol^{-1}, with increasing size,[56] perhaps as a result of increasing dipole−quadrupole and dipole-induced dipole interactions with the polar water solvent.[57] As with alkanes, however, the free energies of solvation and free energy changes are relatively small. Such solvation effects for PAHs in the polar organic solvents normally used in electrochemical experiments might also be expected to be small and to behave similarly as the molecular size increases.[54] Furthermore, the cavitation and dispersion terms for the neutral PAH and ion are likely to nearly cancel in eq 1. Thus, the solvation effects in eqs 1 and 2 are likely dominated by the ionic electrostatic solvation term due to the charge in the anion. We have noted such behavior previously in ammonium and pyridinium ions.[58,59] In our subsequent analysis of the solvation of PAH anions in this paper, the $\Delta\Delta G^\circ_{sol}$ terms for PAHs have then been compared directly with ΔG°_{sol} values for other ions because there are not sufficient experimental data to subtract out the solvation energy of the neutral PAH and the effect of such a subtraction is likely small and regular for a series of PAHs of increasing size.

The large solvation energies for radical anions of PAHs could be modeled using various solvation theories that include electrostatic terms using generalized Born approximations.[55d] We thought that the classical Born electrostatic solvation model,[60] however, might be adapted to these ions to describe their solvation in a much simpler fashion by approximating the PAH ions as spheres of like volume.[61] The Born model predicts that the solvation energies of spherical ions are proportional to the inverse ionic radius (r) according to eq 3, where z is the ionic charge number, e is the electron charge, and D is the dielectric constant.

$$\Delta G^\circ_{sol}(M^{-\bullet}) = -[(z^2e^2)/2r][1 - (1/D)] \quad (3)$$

The Born model has been remarkably successful in predicting trends in solvation energies of spherical alkali metal ions, halide ions, polyvalent ions, and tetraalkylammonium ions.[58,62] The neglect of effects of dielectric saturation and electrostriction in the simple Born model is a possible limitation.[62d,g,h] The success of the method, however, depends most critically upon the choice of the ionic radii.[62a,e,i,j,n] The choice of an effective radius larger than the crystal radius, more in accord with a solvent cavity size, can give good fits to experimental solvation energies.[62e,i,n] Such correlations may also be applied simultaneously to both negative and positive ions with good success. To apply this model to the electrostatic solvation of the radical anions from PAHs requires the assumption that these ions may be approximated as spherical in shape with an effectively uniform charge density distribution. Perusal of the atomic charges in PAH anions shows significant variations from carbon to carbon, but usually a general tendency for the charge densities to become more even when averaged over several adjacent carbons. Furthermore, the calculated dipole moments for the neutral PAHs and their anions are usually similar in magnitude, usually less than 1 D. Thus, effective ionic radii have been derived by treating the ions as spheres with volumes equal to those calculated from the volume calculation option in Gaussian with a B3LYP/6-31+G(d,p) electron-density distribution at the DFT-optimized geometry of the anion using a 0.001 e $bohr^{-3}$ density envelope, or from the PC Model and Sybyl programs for the neutral PAH. All methods of volume calculation correlate very well with one another, with the radii from electron-density volumes of the anions about 2−5% greater than volumes of neutral PAHs from the molecular modeling packages or their B3LYP/6-31+G(d,p) densities.

Half-wave reduction potentials have been measured for a large number of aromatic hydrocarbons[2,21i,51] and are summarized in Table 2. Because of the many experimental conditions under which such measurements have been made, reliable comparisons of trends in such data require attention to the details of solvent, conducting salt concentration, temperature, and reference electrode. The most complete set of data on 40 molecules in the first column of Table 2 comes mainly from the compilation of Mann and Barnes[51a] with a mercury reference electrode, mainly in dimethylformamide solvent with 0.1 M teraalkylammonium salt. Where solvents or conditions varied, care was taken to see that such effects would have a minimal effect, usually less than 0.05 V. Another set of data referenced to the standard calomel electrode (SCE) is tabulated, again mainly with DMF solvent and 0.1 M tetraalkylammonium salt.[2,21i,51] The second set was completed with estimated reduction potentials from the first set with a 0.5 V correction for changing the reference electrode from Hg to SCE. A third set of data from various sources versus SCE was also treated and gives similar results but is not included in Table 2.[51]

In a first attempt to compare gas and solution energies for electron attachment, we carried out simple regression analyses of EA versus reduction potential. This approach has been used in the past to show that the differences in free energies of solvation, $\Delta\Delta G^\circ_{sol}$, can be nearly constant in a series of related molecules, leading to a close correlation between solution and gas-phase data.[21i] In the analysis of Ruoff et al., $\Delta\Delta G^\circ_{sol}$ was found to be nearly constant at 1.99 eV, varying from 1.89 to 2.15 eV for their set of 21 hydrocarbons ranging in size from

benzene to pentacene.[21i] When we expand the range of the sizes of the hydrocarbons treated, however, and use EAs reevaluated in the light of theory, we will conclude that the $\Delta\Delta G^\circ_{sol}$ term cannot generally be assumed to be constant.

Regression analyses between $\Delta G^\circ_{a,298K}$ and $E_{1/2}$ for the 26 best known EAs show a reasonable correlation with $R^2 = 0.8140$ and a standard error in $\Delta G^\circ_{a,298K}$ of 0.18 eV, with maximum errors as large as 0.31 eV. We observed, however, that the regression errors were systematic for large and small molecules in a fashion that indicated that the $\Delta\Delta G^\circ_{sol}$ term is not constant and is largest for the smallest ions. Thus, we hoped to improve this correlation and reduce the residual errors by employing the Born model for the prediction of solvation energies as a function of ionic size. To directly test whether solvation energies could simply be related to ion size, $\Delta\Delta G^\circ_{sol}$ values were calculated from eq 2, with $E_{ref} = -4.21$ V for the Hg electrode and -4.71 V for the SCE electrode.[21i,53b] Perusal of the $\Delta\Delta G^\circ_{sol}$ data in Table 2, where the hydrocarbons are mainly arranged in order of increasing number of carbons, shows that the energies vary with ionic size from -2.69 eV for 1,3-butadiene and cyclobutadiene to -1.88 eV for picene and -1.65 for C_{60} and C_{70}. Thus, the variation in anion solvation energies is 1.04 eV (24 kcal mol^{-1}) compared to a range of 3.42 eV for $\Delta G^\circ_{a,298K}$ and 3.10 V for $E_{1/2}$. This variation is enough to cause problems in a simple linear correlation between $\Delta G^\circ_{a,298K}$ and $E_{1/2}$, particularly since the solvation energy differences, $\Delta\Delta G^\circ_{sol}$, do not correlate well with $\Delta G^\circ_{a,298K}$ or $E_{1/2}$ values, as mentioned above. A tendency for the smallest ions to show larger $\Delta\Delta G^\circ_{sol}$ values is evident in the data. The effective ionic radii from Gaussian electron-density envelope volumes are shown in the right-hand column of Table 2.

Sometimes ionic solvation energies are closely related to ion stabilities, which may, in-turn, be related to ionic size and/or charge delocalization.[21bi,23,52,58,59] This can lead to reasonably good correlations between solution and gas-phase ion stability data, though not always with unit slope. For example, charge delocalization, or effective ionic size, and ionic stability are well-correlated in proton affinities (PAs) for protonation of amines and substituted pyridines, and the ionic solvation energies can also correlate well with PA.[58,59] In Table 2, the electron affinities, or stabilities of the radical anions, however, are not a simple function of the ionic sizes or charge delocalizations in the anions. Regressions between EA and the number of carbons show R^2 values of less than 0.45 and a large scatter in the data. The ion stabilities depend on more subtle quantum mechanical effects associated with the resonance energies of the neutral PAHs and their anions as well as ionic size. For example, the antiaromatic hydrocarbons, pentalene and cyclooctatetraene and, to a lesser extent, cyclobutadiene and biphenylene, show abnormally high electron affinities, partly due to antiaromatic destabilization of the neutral molecule that is apparently partially relieved in the radical anion. Also, the linearly fused PAHs (naphthalene, anthracene, tetracene, and pentacene), as well as azulene and acenaphthylene, have unusually high EAs for their size. Benzene, triphenylene, and coronene have unusually low EAs. Thus, for the EAs of PAHs, an analysis of the solvation energies appears to require an approach, such as that in the Born model, that more explicitly accounts for variation in the solvation energies of the anions.

Testing the Born Model. To quantitatively test the predictions of the Born model, regressions were carried out for the variation of $\Delta\Delta G^\circ_{sol}$ with an effective ionic radius according to eq 3, making use of the 26 most reliably known experimental EAs, and excluding those molecules whose EAs are estimated and quoted to only one decimal accuracy in Table 2. At first a regression of $\Delta\Delta G^\circ_{sol}$ with the inverse of the cube root of the number of carbons was tried with success and an R^2 of 0.9160.[61] A regression between $\Delta\Delta G^\circ_{sol}$ and $1/r$ using the effective ionic radius from ionic volumes from B3LYP/6-31+G(d,p) density envelopes shown in Table 2 gives a good correlation (eq 4) with $R^2 = 0.9138$ and a standard error in $\Delta\Delta G^\circ_{sol}$ of 0.073 eV, not much larger than the uncertainties in the reduction potentials or the electron-attachment energies. Similar statistical results are exhibited for the second set experimental reduction potentials referenced to SCE with a standard error of 0.087 eV. Effective PAH radii from the PC Model (or Sybyl) modeling program give regressions almost identical to those with radii based upon electron densities, $R^2 = 0.9035$. The simple Born model, then, provides a major improvement in the prediction of solvation energies compared to the 1.04 eV variation found when the solvation energies are assumed to be constant.

$$\Delta\Delta G^\circ_{sol}\,(\text{eV}) = -6.0040(1/r) - 0.644 \qquad (4)$$

The solvation energies predicted from the regression expressed in eq 4 can be combined with experimental solution reduction potentials versus Hg in eq 2 to give the predicted gas-phase free energy values for electron attachment, $\Delta G^\circ_{a,pred}$, found in Table 2. For the 26 molecules that formed the basis of the regression in eq 4, the differences between the experimental and predicted values of $\Delta G^\circ_{a,298K}$ are tabulated as the residual errors in y. These residual errors are identical to the residual errors for the prediction of $\Delta\Delta G^\circ_{sol}$ from the regression with $1/r$ in eq 4. They show that there are no major outliers in the regression with almost all residual errors less than 0.10 eV. The $\Delta G^\circ_{a,pred}$ values for the other hydrocarbons provide an indirect, but apparently accurate, measure of their gas-phase electron-attachment energies that have been used to estimate $G^\circ_{a,298K}$ values in Tables 1 and 2 for the 16 molecules not included in the regression whose experimental data were missing or suspect.

For four molecules (1,3,5-tri-*tert*-butylpentalene, pentalene, **1**, and cyclobutadiene), there are no experimental gas-phase EA measurements. The instabilities of the antiaromatic molecules, cyclobutadiene and pentalene, have precluded the measurement of reduction potentials or EAs, but these experimental quantities may now be predicted using eq 4 and other data as discussed in more detail later.

For 14 hydrocarbons whose experimental gas-phase experiments were suspect (styrene, indene, biphenylene, biphenyl, fluorene, phenanthrene, the methylnaphthalenes, acenaphthylene, 1,1-diphenylethylene, fluoranthene, corannulene, perylene, and benzo[ghi]perylene), the predicted $\Delta G^\circ_{a,pred}$ values from the Born model were used to pick recommended values in place of gas-phase experimental data, $\Delta G^\circ_{a,298K}$, in Table 2 or to aid in picking the most reliable of several different experimental values (benz[*a*]anthracene, benzo[*c*]phenanthrene, and dibenz[a,j]anthracene). The nominal experimental EA_{exptl} and other experimental values in Table 2 are estimated from these solution values combined with theoretical zero-point energy and thermal and entropy terms.

For cyclobutadiene, the predicted $-\Delta G^\circ_{a,298K}$ value of -0.13 eV from the literature reduction potential is in close agreement with the high-level theoretical value used in place of an experimental value in Table 2 (vide infra). The methylnaphthalenes were assigned estimated values identical to that for naphthalene based upon the fact that methyl substituent effects are expected to be very small, for example, for 1-methylanthracene and from known reduction potential data.[2,51] As discussed later, the experimental EAs for phenanthrene and

fluoranthene are close to predictions from reduction potentials and quantum theory.

To see if the solvation energies predicted by the regression in eq 4 are physically reasonable, we made comparisons with solvation energies of a series of spherical alkali metal and alkylammonium cations and halide anions. To directly compare the $\Delta\Delta G°_{sol}$ values from PAHs with free energies of aqueous solvation, one must consider the effects of changing solvent and the effect of the neutral free energy of solvation on the $\Delta\Delta G°_{sol}$ term. Most of the reduction potentials were measured in DMF. The effect of the change in dielectric constant from water to DMF ($D = 38.25$) for $E_{1/2}$ data would be nearly negligible, 1.5% in the $[1 - 1/D)]$ term. What about the role of the neutral solvation on $\Delta\Delta G°_{sol}$? The neutral PAH solvation free energies are not widely available,[54] but what data exist and the predominance of the electrostatic term in ions[58,59] suggest that $\Delta\Delta G°_{sol}$ values can be meaningfully compared with $\Delta G°_{sol}$ values for other ions as discussed above.

Thus, we have included the $\Delta\Delta G°_{sol}$ terms for PAHs with free energies of solvation of other anions and cations on the same solvation energy scale for comparison with ionic radius data according to the Born model.[58,62] We have used the same ionic radius scale from DFT electron densities for the alkali metal and halide ions as used for the PAH anions to achieve a consistently determined set of radii for all ions, even though other ionic radius scales are known to give better correlations within the Born model. A regression of aqueous free energies of solvation, $-\Delta G°_{sol}$, with $1/r$ that includes only solvation data for effectively spherical ions (alkali metal and halide ions, ammonium ion, and two tetraalkylammonium ions)[62l,n] gives $R^2 = 0.9062$ with a standard error of 4.8 kcal mol^{-1}, a slope of 129.0 kcal mol^{-1} Å, and an intercept of 13.4 kcal mol^{-1}. Outlier points for fluoride, lithium, and sodium were excluded. A regression including these nine ions and the 42 PAHs and other molecules from Table 2 gives $R^2 = 0.9440$ with a standard error of 2.4 kcal mol^{-1}, a slope of 115.2 kcal mol^{-1} Å, and an intercept of 20.7 kcal mol^{-1}. The smallest ions are again outliers in such a regression. Fluoride ion's solvation energy lies about 25 kcal mol^{-1} above the plot, and the points for lithium and sodium ion are low by 10 and 3 kcal mol^{-1}, respectively. When only negative ions are included in the regression, chloride, bromide, and iodide and the 42 molecules in Table 2, the regression shows $R^2 = 0.9416$ with a standard error of 1.73 kcal mol^{-1}, a slope of 138.3 kcal mol^{-1} Å, and an intercept of 15.1 kcal mol^{-1}. A plot of this correlation is shown in Figure 1. The Born model predicts a slope of 163.9 kcal mol^{-1} Å and zero intercept for water solvent. When the data for Figure 1 are treated in a regression enforcing a zero intercept, the fit is worse, with a standard error of 3.6 kcal mol^{-1} and a slope of 193 kcal mol^{-1} Å. While the slopes and intercepts from the Born model are not quantitatively correct and vary for different classes of molecules, the model is useful in predicting absolute and relative solvation energies for the PAHs and is reasonably consistent with solvation energies of various spherical anions and cations. Further studies to better define the effects of neutral solvation energies and of PAH anion shape and charge distribution may add to this picture.

Solvation of C_{60}^- and C_{70}^-. Included in the data set for Figure 1 are the two fullerenes, C_{60} and C_{70} from Table 2. The EAs for C_{60} (2.689 eV) and C_{70} (2.676 eV) were measured by the LPES method.[63] Reduction potentials for C_{60} and C_{70} in the literature are also very similar to one another.[21i,64] The reduction potentials in DMF for both C_{60} and C_{70} are -0.26 V vs SCE (0.26 V vs Hg).[21i,64b] In other solvents, reduction

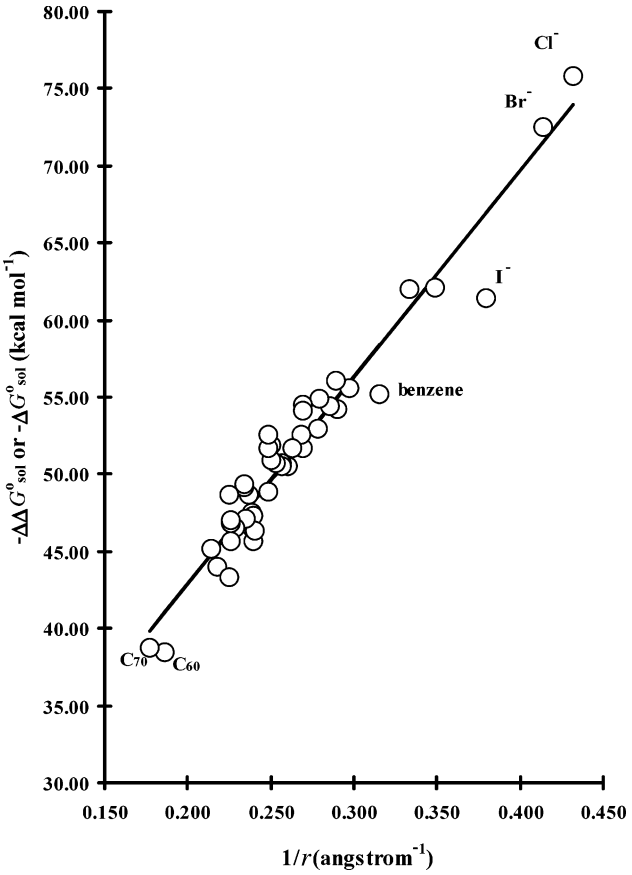

Figure 1. Born plot of negative free energies of solvation of PAH anions and halides versus inverse ionic radius (l/*r*).

potentials (in volts) for C_{60} versus SCE (with the solvent and its dielectric constant in parentheses) are -0.36 (benzene, 2.28), -0.39 (chlorobenzene, 5.62), -0.33 (THF, 7.58), -0.39 (*o*-dichlorobenzene, 9.93), -0.49 (dichloromethane, 9.10), -0.48 (1,2-dichloroethane, 10.37), -0.34 (pyridine, 12.91), -0.42 (benzonitrile, 25.20), -0.44 (nitrobenzene, 34.78), and -0.26 (DMF, 36.71).[21i,64b] Reduction potentials with other reference electrodes give similar results when corrected to the SCE reference.[64] The reduction potential data show a very rough correlation with the dielectric constant function, $1 - 1/D$ ($R^2 = 0.148$, excluding benzene), with the changes of a magnitude consistent with predicted changes in solvation energy from simple Born theory. A better correlation ($R^2 = 0.471$) with $1 - 1/D$ is found with the difference in reduction potential relative to that for an internal ferrocene/ferrocenium internal standard, especially when the outlier solvent benzene is excluded. Such a correlation with electron-acceptor properties of the solvents as expressed in the normalized Dimroth−Reichardt solvent parameter, $E_T^N(30)$, has been previously noted ($R^2 = 0.300$), though not as strong as with $1 - 1/D$.[64b]

Using thermal and entropy terms from B3LYP/6-31G(d) frequency calculations and the experimental EA, the experimental $-\Delta G°_{a,298K}$ value for C_{60} is estimated at 2.78 eV, and that for C_{70} probably very similar. A very different EA of 1.62 eV has also been measured by the kinetic method (CID), and this discrepancy was attributed to a "local" EA in C_{60}.[25a] The literature data in the gas phase and solution for C_{70} are very similar to those for C_{60}.[21i,63,64] The data points for C_{60} and C_{70} in Figure 1 are below the correlation line by only 2.6 and 1.1 kcal mol^{-1}, respectively. Thus the Born model nicely relates the solvation behavior of these ions to the other PAHs.

Theoretical Approaches for Predicting EAs. In Table 3 are comparisons of results from different Koopmans' Theorem-type methods, including a propagator method, the outer-valence Green's Function (OVGF) approximation. The simplest method consists of performing a geometry optimization on the neutral hydrocarbons and using the LUMO energy as an approximation of the EA. These results are listed in Table 3 under $E_{LUMO}(M)$ for various basis sets. Although Koopmans' approximation often provides reasonable estimates of ionization potentials, including for PAHs, due to a fortuitous cancellation of errors,[65] it usually fails to provide reasonable estimates of absolute values of electron affinities. It can be effective, however, in reproducing the trends in electron-attachment energies of hydrocarbon molecules.[26a] All of the HF-calculated values are 2−3 eV more negative than the experimental EAs, while the DFT values are too positive. Nevertheless, the experimental trends are roughly reproduced by all of the types of calculations. A comparison of the effectiveness of different theoretical methods in reproducing trends in the experimental EAs can be drawn from the EAs relative to benzene shown in the second row for each method. Curiously, the inclusion of diffuse functions appears to give a poorer reproduction of experimental trends than any of the other methods.

Another calculational approach is to treat the radical anion at the neutral or anion geometry using Koopmans' Theorem to approximate the EA from the HOMO energy of the radical anion. These results are listed under $E_{HOMO}(M^-)$ with various basis sets. Again, the absolute values are far from the experimental ones, but the trends are approximately reproduced by both HF and DFT methods. The choice of the optimized neutral or radical anion geometry or basis set makes relatively little difference in the energy differences, although the absolute values are affected.

A propagator method, the outer valence Green's Function approximation, has been used with the 6-311G(d,p) basis set to calculate the EA of the neutral species. The OVGF approximation explicitly calculates terms in the electron-propagator method up to third order and includes an estimate of fourth- and higher-order terms. For the entries in Table 3, the corrections are in the right direction compared with the $E_{LUMO}(M)$ with the 6-311G(d,p) basis set but still far from experiment. The experimental differences, however, are reproduced only about as well as by the other Koopmans' methods. A more extensive comparison of results from Koopmans' methods will be presented and discussed later.

These Koopmans' methods have the advantage over the more direct calculation of neutral/anion energy differences (ΔE method) of requiring only a single calculation. Despite the potential problems from electron-correlation errors, geometry relaxation effects, and spin contamination inherent in the calculation of energy differences between neutral and radical anion states, "ΔE" calculations have the potential to provide more accurate absolute values and trends in energy differences than found for the Koopmans' methods. In Table 4 are some comparisons of these different theoretical methods for a larger set of PAHs and related molecules.

Spin contamination in the radical anions was found to be considerable using the UHF method, with $<S^2>$ values ranging from 0.8229 for biphenylene to 2.2797 for picene, where the doublet states are expected to have an $<S^2>$ value of 0.7500. Møller−Plesset perturbation theory calculations give similarly less spin contamination with $<S^2>$ values (see Supporting Information). Remarkably, the density functional calculations gave much less spin contamination, with $<S^2>$ ranging from 0.7523 for cyclobutadiene to 0.7639 for pentacene and to 0.7709 for pentalene at the UB3LYP/6-311G(d,p) level, and from 0.7528 for cyclooctatetraene to 0.7646 for pentacene and to 0.7709 for pentalene at the UB3LYP/6-31+G(d,p) level. When restricted open-shell DFT [ROB3LYP/6-311G(d,p)] calculations were performed on several PAH anions, the energies were increased compared to UB3LYP results, but by only 0.02−0.04 eV, indicating a small energetic effect for spin contamination.

How such dramatic differences in spin contamination affect the reaction energetics is evident in the comparisons between experiment and EA values found in Table 4. Comparisons of $<S^2>$ values for UHF and UMP2 calculations are tabulated in Tables S2 and S3 of the Supporting Information. The 10 hydrocarbons represented in Table 4 are of a size small enough that MP2 calculations and DFT calculations with a very large basis set were practical. Included in this set are a number of unusual molecules of highly strained and/or antiaromatic electronic structure that may pose special problems theoretically and experimentally. These molecules were included as comparison cases because of suspicions that the value for the experimental EA for biphenylene, which is both strained and antiaromatic, might be incorrect. The calculated absolute EAs in Table 4 and differences in the values relative to benzene are compared with experimental results, as in Table 3. The calculated EAs used in this table are "electronic" EA values, $-\Delta E^\circ_{a,e}$, with no zero-point energy or thermal energy corrections. The experimental EAs based upon free energies are "back corrected" using DFT-calculated zero-point energy, thermal energy, and entropy terms, as appropriate, to give experimental $-\Delta E^\circ_{a,e}$ values for direct comparison with theory.

The absolute EAs from the ΔE method in Table 4 are in closer absolute agreement with experiment than those from Koopmans' methods in Table 3, particularly those values from the DFT method and to a lesser extent the MP2 method. The HF method gives absolute values that are too negative, presumably because electron-correlation effects in the radical anion are not accounted for, thus making all of the EAs too negative. The MP2 results suffer from a similar problem. Spin contamination plays an additional role in reducing the accuracy of the HF or MP2 results and is discussed later. Increasing the size of the basis set and inclusion of diffuse functions improve the absolute agreement substantially for the HF method. Such an effect of basis set is also seen for the DFT method, but with the increases in the EA values essentially converging at the 6-31+G(d,p) and larger basis sets. Although the B3LYP/6-311G(d,p) data do not agree in absolute values as well as the B3LYP/6-31+G(d,p) results, the relative values appear similar from the data in Table 4. EAs were calculated for set of 27 PAHs at the B3LYP/6-311+G-(2df,2pd) and found to be larger than at the B2LYP/6-31+G-(d,p) values only by 0.01−0.05 eV, except that the cyclobutadiene and indene values were lower by 0.01 and 0.02 eV, respectively.

For 1,3-butadiene and cyclobutadiene, the EA calculations were carried out at an effectively very high level, CCSD(T)/cc-aug-pVTZ//B3LYP/6-31+G(d,p) using G2(MP2)-type additivity methods from CCSD(T)/6-31+G(d,p) and MP2/cc-aug-pVTZ calculations. At this level, it is expected that the theoretical energies would have converged to within 0.1 eV or better,[48a,b] except for spin-contamination corrections, which could raise the EAs by 0.159 and 0.063 eV for 1,3-butadiene ($<S^2>$ = 0.8346) and cyclobutadiene ($<S^2>$ = 0.7772), respectively. These corrections, as determined by the PMP2 method at the MP2/cc-aug-pVTZ level, are maximum values since further reduction in spin contamination might be expected

in the CCSD(T) calculations. Spin-contamination corrections are, therefore, not reflected in the tabulated values, and their effect in raising the calculated EA is expected to be quite small. In fact, the theoretical attachment energy and experimental electronic EA, $-\Delta E^\circ_{a,e}$, for 1,3-butadiene agree within 0.04 eV, although the ETS electron-attachment energy may not represent a true adiabatic EA. To test this, we estimated the vibrational relaxation energy as the difference in energy between the radical anion at the neutral geometry, a "vertical" transition, and the radical anion at the optimized geometry. At effectively the CCSD(T)/cc-aug-pVTZ level, this relaxation energy was only 0.15 eV for 1,3-butadiene. In the comparison between theory and experiment, these two effects of spin contamination (<0.159 eV) on the theoretical EA and the lack of vibrational relaxation (ca. 0.15 eV) in the ETS value are estimated to both be small and of similar magnitude. Since inclusion of these corrections would tend to make both the theoretical and experimental $-\Delta E^\circ_{a,e}$ values slightly more positive, the good agreement between the two should be expected to survive such considerations. Addition of the calculated zero-point energy correction leads to an expected theoretical EA at 0 K of −0.57 to −0.67 eV, about 0.05 eV lower than the experimental $-\Delta E^\circ_{a,e}$ value of 0.68 eV used in Table 2.

The EA for cyclobutadiene can be estimated from an experimental reduction potential of the dithio derivative **1**.[51b,66] From the success with butadiene, however, we expected that the CCSD(T) calculated $-\Delta E^\circ_{a,e}$ of −0.15 eV and $-\Delta G^\circ_{a,298K}$ of −0.08 eV (Tables 2 and 4) would be more accurate than the experimental prediction from reduction potentials. The theoretical value should presumably be less negative when correction for spin contamination is included, but by less than 0.06 eV (vide supra). It has previously been suggested from Koopmans' Theorem predictions that the EA for cyclobutadiene is likely negative.[67] If the value of −0.08 eV is used for $-\Delta G^\circ_{a,298K}$ for cyclobutadiene, then our Born model estimate of solvation energies would lead to a predicted reduction potential of −1.6 V versus Hg in DMF. In apparent agreement, an estimated reduction potential for cyclobutadiene of −1.6 eV appears in the literature based upon a value of −2.0 V versus Hg for **1**, but how this was estimated is not clear.[51b] As we shall see, DFT methods predict that the $-\Delta G^\circ_{a,298K}$ for cyclobutadiene should be 0.56 eV less than **1**. Combining this difference with our Born model estimate of 0.25 eV for $-\Delta G^\circ_{a,298K}$ for **1**, we would predict a $-\Delta G^\circ_{a,298K}$ value of −0.26 for cyclobutadiene, which agrees moderately well with the value of −0.08 eV from high-level theory. This, in turn, leads to a predicted reduction potential of about −1.7 eV for cyclobutadiene, again using the Born model.

The trends in experimental $-\Delta E^\circ_{a,e}$ values relative to benzene in Table 4 are reproduced by the HF data about as well as Koopmans' Theorem data from Table 3, but inclusion of electron-correlation effects at the MP2 or DFT levels leads to much-improved agreement. For the DFT calculations, the agreement generally improves somewhat as diffuse functions are added to the basis set. The convergence with larger basis sets noted earlier for absolute EA values and a similar convergence for the energy differences support the use of the B3LYP/6-311G(d,p) or B3LYP/6-31+G(d,p) as a reasonable compromise for the economical calculation of $-\Delta E^\circ_{a,e}$ values for larger PAHs. Except for pentalene, the agreement in the energy differences from benzene is generally within 0.2 eV at DFT levels. This suggests that the estimated EA for pentalene from reduction potentials may be too low and will be looked at more closely (vide infra). Similarly, the experimental $-\Delta E^\circ_{a,e}$ of 0.74 eV for biphenylene from collisionally induced dissociation (CID) mass spectrometry is apparently too high, while the estimate of 0.1 eV from reduction potentials is within 0.1 eV of the better theoretical values, theoretical methods that well reproduce $-\Delta E^\circ_{a,e}$ values of other strained and antiaromatic molecules.

The MP2-calculated $-\Delta E^\circ_{a,e}$ differences agree with experimental differences nearly as well as those from DFT calculations. Azulene and cyclobutadiene are cases where the MP2 calculations are in largest disagreement with the most accurate estimates of the experimental differences. Azulene is a molecule whose radical anion shows one of the largest MP2 spin contamination problems ($<S^2> = 1.0670$), which might help account for the larger disagreement with experiment. When PUMP2 calculations on the anion are used to help remove the spin contamination, however, we see much better agreement with experiment. Cyclobutadiene anion, on the other hand, shows little spin contamination and still does not agree very well, with or without spin annihilation. HF and MP2 methods are tested further and discussed subsequently in connection with Table 6.

For calculation of EAs on the full set of 45 PAHs and related compounds up to 60 carbons, the HF/6-311G(d,p), B3LYP/6-311G(d,p), and B3LYP/6-31+G(d,p) methods were chosen as realistically possible and reasonably accurate. These data are summarized in Table 5. Included in the table are calculated electronic $-\Delta E^\circ_{a,e}$ values and calculated enthalpies and free energies for electron attachment at room temperature labeled as $-\Delta H^\circ_{a,298K}$ and $-\Delta G^\circ_{a,298K}$, respectively, along with experimental free energy values, $\Delta G^\circ_{a,298K}$. Results of regression analyses of experimental and theoretical values are summarized at the bottom of the table. The regression statistics, R^2, and the regression constants, m and b, are shown at the bottom of Table 5 beneath the appropriate columns of theoretical data for a linear regression, $y = mx + b$, with the experimental values as y. Residual regression errors in y for individual data points are listed in columns at the right side of Table 5 for the HF/6-311G(d,p), B3LYP/6-311G(d,p), and B3LYP/6-31+G(d,p) calculations of $\Delta G^\circ_{a,298K}$ in order to see which hydrocarbons show the largest deviations from the regression and might present special problems in the theory or experiment.

The predicted values for $\Delta G^\circ_{a,298K}$ from the B3LYP/6-31+G(d,p) theoretical method and regression equation are tabulated in the column immediately following the experimental data, followed by the residual deviations from the best-fit line. The signs of the errors are then such that, when added to the theoretically predicted values, they reproduce experiment. The next column of residual errors is for a regression of experimental free energies and calculated electronic energies to see the effects of the zero-point energy and thermal and entropy corrections. The standard error increases from 0.070 to 0.077 eV when calculated electronic energies are used instead of free energies. Differences in the residual errors are generally small but substantial in certain cases, such as coronene. The overall regression statistics are only slightly inferior to that with the free energy that includes all of these corrections. The HF results give an inferior regression fit with the standard error rising to 0.130 eV. Nevertheless, the quality of the fit is reasonably good, considering the potential problems with spin contamination and poor absolute agreement between experiment and theory.

The DFT regressions show remarkably good fits with experiment, with both the B3LYP/6-311G(d,p) and B3LYP/6-31+G(d,p) methods giving similar regression statistics and nearly identical standard errors of 0.077 and 0.070 eV,

TABLE 5: Experimental and Theoretical Adiabatic Electron-Attachment Energies, Enthalpies, and Free Energies by the ΔE Method and Linear Regression Results (all values in electronvolts)

										Residual Regression Errors in *y*			
	HF/6-311G(d,p)	B3LYP/6-311G(d,p)				B3LYP/6-31+G(d,p)		exptl	B3LYP/6-31+G(d,p)			HF/6-311G(d,p)	B3LYP/6-311G(d,p)
	$-\Delta E°_{a,e}$	$-\Delta E°_{a,e}$	$-\Delta E°_{a,0K}$	$-\Delta H°_{a,298K}$	$-\Delta G°_{a,298K}$	$-\Delta E°_{a,e}$	$-\Delta G°_{a,298K}$	$-\Delta G°_{a,298K}$	$-\Delta G°_{a,pred}$[a]	$-\Delta G°_{a,298K}$	$-\Delta E°_{a,e}$	$-\Delta E°_{a,e}$	$-\Delta G°_{a,298K}$
benzene	−2.54	−1.68	−1.40	−1.45	−1.33	−1.32	−0.97	−1.04	−0.98	−0.06	0.00	−0.18	−0.02
benzocyclobutadiene	−1.09	0.00	0.14	0.12	0.16	0.25	0.41	0.29	0.29	0.00	−0.03	0.10	0.07
styrene	−1.47	−0.53	−0.37	−0.38	−0.36	−0.25	−0.08	−0.1[b]	−0.16	0.06	0.01	−0.02	0.11
cyclooctatetraene	−0.72	0.59	0.66	0.66	0.67	0.81	0.89	0.66	0.73	−0.07	−0.14	0.20	0.01
azulene	0.08	0.46	0.59	0.58	0.61	0.65	0.80	0.81	0.65	0.16	0.14	−0.24	0.21
naphthalene	−1.47	−0.42	−0.25	−0.27	−0.22	−0.24	−0.04	−0.16	−0.12	−0.04	−0.06	−0.07	−0.06
1-Menaphthalene	−1.47	−0.40	−0.23	−0.24	−0.20	−0.22	−0.02	−0.2	−0.11	−0.09	−0.11	−0.12	−0.12
2-Menaphthalene	−1.49	−0.43	−0.26	−0.27	−0.23	−0.20	0.00	−0.2	−0.09	−0.11	−0.13	−0.10	−0.09
acenaphthylene	−0.13	0.57	0.69	0.69	0.72	0.73	0.87	0.8[b]	0.72	0.08	0.07	−0.09	0.12
biphenylene	−1.26	0.00	0.14	0.13	0.15	0.16	0.32	0.2[b]	0.20	0.00	−0.04	0.13	−0.01
biphenyl	−1.32	−0.37	−0.21	−0.23	−0.16	−0.16	0.05	−0.1[b]	−0.04	−0.06	−0.06	−0.13	−0.05
fluorene	−1.39	−0.47	−0.30	−0.32	−0.27	−0.29	−0.09	−0.1[b]	−0.17	0.07	0.05	−0.07	0.04
anthracene	−0.66	0.42	0.56	0.55	0.58	0.55	0.71	0.60	0.57	0.03	0.02	0.09	0.03
phenanthrene	−1.13	−0.18	−0.01	−0.03	0.03	−0.03	0.17	0.1[c]	0.07	0.03	0.03	−0.06	−0.01
diphenylacetylene	−0.78	0.19	0.33	0.32	0.34	0.33	0.48	0.32	0.35	−0.03	−0.07	−0.10	−0.05
trans-stilbene	−0.59	0.29	0.43	0.42	0.37	0.45	0.53	0.35	0.40	−0.05	−0.14	−0.21	−0.05
1,1-diphenylethylene	−1.24	−0.16	−0.01	−0.02	−0.01	0.02	0.17	0.2[b]	0.07	0.13	0.08	0.12	0.12
1-Meanthracene	−0.66	0.41	0.56	0.54	0.58	0.54	0.70	0.55	0.56	−0.01	−0.01	0.04	−0.02
fluoranthene	−0.19	0.60	0.74	0.73	0.76	0.74	0.89	0.7[d]	0.73	−0.03	−0.04	−0.15	−0.02
pyrene	−0.66	0.31	0.46	0.44	0.48	0.43	0.60	0.56	0.46	0.10	0.09	0.06	0.07
benz[*a*]anthracene	−0.50	0.47	0.62	0.61	0.65	0.58	0.76	0.70	0.61	0.09	0.09	0.08	0.07
benzo[*c*]phenanthrene	−0.94	0.22	0.39	0.38	0.42	0.34	0.53	0.40	0.40	0.00	0.00	0.10	−0.03
chrysene	−1.02	0.18	0.36	0.34	0.41	0.31	0.53	0.42	0.40	0.02	0.05	0.17	−0.01
naphthacene(tetracene)	−0.06	1.00	1.12	1.12	1.15	1.09	1.23	1.02	1.04	−0.02	−0.03	0.07	−0.02
triphenylene	−1.12	−0.13	0.11	0.08	0.18	0.03	0.34	0.29	0.22	0.07	0.17	0.12	0.05
benzo[*a*]pyrene	−0.11	0.68	0.82	0.81	0.85	0.79	0.95	0.77	0.78	−0.01	−0.01	−0.14	−0.03
benzo[*e*]pyrene	−0.71	0.34	0.50	0.49	0.54	0.47	0.67	0.49	0.53	−0.04	−0.02	0.02	−0.04
perylene	0.06	0.84	0.98	0.97	1.01	0.98	1.14	1.00	0.96	0.04	0.06	−0.03	0.07
benzo[ghi]perylene	−0.30	0.64	0.78	0.77	0.81	0.75	0.92	0.7[b]	0.76	−0.06	−0.05	−0.07	−0.06
pentacene	0.39	1.42	1.53	1.52	1.55	1.49	1.63	1.32	1.41	−0.09	−0.07	0.05	−0.06
picene	−0.45	0.31	0.47	0.46	0.53	0.42	0.64	0.54	0.50	0.04	0.08	−0.12	0.01
dibenz[a,h]anthracene	−0.80	0.51	0.67	0.66	0.70	0.61	0.80	0.68	0.65	0.03	0.05	0.28	0.01
dibenz[a,j]anthracene	−0.81	0.49	0.67	0.65	0.70	0.60	0.81	0.60	0.66	−0.06	−0.03	0.20	−0.07
coronene	−0.61	0.41	0.68	0.64	0.78	0.49	0.86	0.57	0.71	−0.14	0.05	0.03	−0.17
1,3-butadiene	−1.91	−1.00	−0.81	−0.84	−0.76	−0.59	−0.35	−0.64	−0.41	−0.23	−0.23	−0.23	−0.09
cyclobutadiene	−1.49	−0.43	−0.28	−0.31	−0.21	0.02	0.24	−0.08[e]	0.14	−0.22	−0.20	0.02	0.01
pentalene	0.37	1.09	1.22	1.22	1.24	1.33	1.48	1.4[f]	1.27	0.13	0.15	0.14	0.28
indene	−1.84	−0.83	−0.62	−0.64	−0.60	−0.59	−0.35	−0.4[b]	−0.41	0.01	0.01	−0.05	0.01
corannulene	−0.16	0.50	0.70	0.67	0.83	0.63	0.96	0.8[b]	0.79	0.01	0.15	−0.07	0.02
C_{60}		2.52	2.71	2.66	2.80	2.99	3.27	2.78	2.92	−0.14	0.09		0.36
1		0.67	0.76	0.77	0.76	0.77	0.86	0.3[b]	0.70	−0.40	−0.47		−0.42
2		0.19	0.31	0.31	0.31	0.33	0.45		0.33				
3		0.76	0.86	0.86	0.86	0.91	1.01		0.84				
1,3,5-tri-*t*-Bupentalene		1.19	1.32	1.32	1.32	1.26	1.39	1.3[b]	1.19	0.11	0.11		0.11
1,3,5-triMepentalene		0.85	1.00	0.98	1.09	1.01	1.25	1.1[f]	1.06	0.04	0.13		0.10
					regression statistics:								
R^2	0.9193				0.9716	0.9714	0.9765						
standard error (eV)	0.130				0.077	0.077	0.070						
N	34				34	34	34						
slope (*m*)	0.7297				0.8334	0.8648	0.9188						
intercept (*b*)	0.987				0.087	0.101	−0.070						
std error in *m*	0.0382				0.0252	0.0262	0.0252						
std error in *b*	0.038				0.016	0.016	0.018						

[a] Predicted free energy from linear regression and calculated B3LYP/6-31+G(d,p) free energy. Residual errors below the bold line are outliers not included in the regression. [b] Experimental free energy suspect. Estimated from reduction potential (vs Hg) and solvent effect with regression with $1/r$ (see Table 1). [c] A value of 0.1 eV better fits the estimated value from reduction potential data in Table 2, the DFT-calculated values, and data in Table 7. [d] A value of 0.7 eV better fits the estimated value from reduction potential data in Table 2, the DFT-calculated values, and data in Table 7. [e] From CCSD(T)-calculated value. [f] Estimated from the 1,3,5-tri-*t*-bupentalene value and DFT-calculated differences.

respectively. An average absolute residual error of 0.05 eV and maximum errors of 0.13 and 0.14 eV are obtained at the preferred B3LYP/6-31+G(d,p) level. The B3LYP/6-311G(d,p) method performs almost as well as the B3LYP/6-31+G(d,p) method, although inclusion of diffuse functions would seem to be important for the proper description of the radical anions. The B3LYP/6-31+G(d,p) calculations give absolute electron-attachment energies that are closer to DFT results with larger basis sets, as noted in Table 4. The experimental energies often lie between the absolute B3LYP/6-311G(d,p) and B3LYP/6-31+G(d,p) values. The B3LYP/6-311G(d,p) values are usually somewhat closer to experiment than the B3LYP/6-31+G(d,p) values, with average absolute errors of 0.09 and 0.13 eV, respectively. The predicted free energies from regressions with

TABLE 6: Experimental and PUHF and PUMP2 Theoretical Adiabatic EAs by the Δ*E* Method with Spin Annihilation[a]

	PUHF/6-31G(d)		PUMP2/6-31G(d)		PUHF/6-31+G(d,p)	PUMP2/6-31+G(d,p)		Exptl	regression error in *y* PUMP2 6-31G(d)
	$-\Delta E^\circ_{a,e}$	$-\Delta G^\circ_{a,298K}$	$-\Delta E^\circ_{a,e}$	$-\Delta G^\circ_{a,298K}$	$-\Delta E^\circ_{a,e}$	$-\Delta E^\circ_{a,e}$	$-\Delta G^\circ_{a,298K}$	$-\Delta G^\circ_{a,298K}$	$-\Delta G^\circ_{a,298K}$
benzene	−2.58	−2.23	−2.68	−2.33	−2.01	−1.79	−1.44	−1.04	−0.26
benzocyclobutadiene	−1.21	−1.04	−0.89	−0.73	−0.66	−0.17	0.00	0.29	0.04
styrene	−1.18	−1.00	−1.59	−1.42	−0.91	−0.87	−0.70	−0.1[b]	0.09
cyclooctatetraene	−0.86	−0.78	−0.36	−0.28	−0.43	0.26	0.34	0.66	0.13
azulene	0.62	0.77	−0.49	−0.34	0.79	0.09	0.24	0.81	0.32
naphthalene	−1.44	−1.24	−1.38	−1.18	−1.02	−0.72	−0.52	−0.16	−0.12
1-Menaphthalene	−1.47	−1.27	−1.30	−1.10				−0.2	−0.21
2-Menaphthalene	−1.48	−1.28	−1.33	−1.14				−0.2	−0.18
acenaphthylene	0.74	0.88	−0.29	−0.14				0.8[b]	0.18
biphenylene	−1.33	−1.18	−0.84	−0.69	−0.89	−0.21	−0.06	0.2[b]	−0.07
biphenyl	−0.55	−0.35	−1.46	−1.25				−0.1[b]	−0.01
fluorene	−0.64	−0.44	−1.49	−1.29				−0.1[b]	0.01
anthracene	−0.61	−0.44	−0.37	−0.20				0.60	0.02
phenanthrene	−0.32	−0.11	−1.18	−0.97				0.1[b]	0.01
diphenylacetylene	0.67	0.82	−0.92	−0.78				0.32	0.10
trans-stilbene	0.80	0.87	−0.71	−0.64				0.35	0.04
1,1-diphenylethylene	0.01	0.16	−1.29	−1.14				0.2[b]	0.22
1-Meanthracene	−0.57	−0.41	−0.40	−0.24				0.55	−0.01
fluoranthene	0.84	0.99	−0.27	−0.12				0.7[b]	0.06
pyrene	−0.21	−0.04	−0.46	−0.29				0.56	0.03
benz[*a*]anthracene	0.67	0.85	−0.70	−0.52				0.70	0.32
benzo[*c*]phenanthrene	−0.71	−0.52	−0.69	−0.50				0.54	0.00
chrysene	1.01	1.23	−0.68	−0.45				0.42	−0.01
naphthacene	0.06	0.21	0.29	0.44				1.02	0.03
triphenylene	0.08	0.39	−1.13	−0.82				0.29	0.10
corannulene	3.12	3.45	0.47	0.79				0.8[b]	−0.42
benzo[*a*]pyrene	1.89	2.06	0.01	0.17				0.77	−0.05
benzo[*e*]pyrene	−0.17	0.03	−0.45	−0.26				0.49	−0.06
perylene	1.97	2.14	0.28	0.45				1.00	0.00
benzo[ghi]perylene	1.01	1.17	−0.09	0.08				0.7[b]	−0.07
pentacene	0.58	0.71	0.78	0.91				1.32	0.02
dibenz[a,j]anthracene	−0.82	−0.61	−0.26	−0.05				0.60	−0.08
coronene	0.43	0.80	−0.35	0.02				0.57	−0.15
1,3-butadiene	−1.95	−1.72	−2.01	−1.78	−1.40	−1.11	−0.87	−0.64	−0.22
cyclobutadiene	−1.76	−1.54	−1.31	−1.09	−1.03	−0.26	−0.04	−0.08[c]	−0.10
pentalene	0.79	0.94	0.40	0.55	1.28	1.06	1.21	1.4[b]	0.34
indene	−1.55	−1.31	−1.83	−1.59				−0.4[b]	−0.10
picene	3.33	3.55	0.52	0.74				0.54	−0.65
dibenz[a,h]anthracene	2.70	2.89	0.27	0.46				0.68	−0.33
				regression statistics					
R^2		0.4805		0.8939					
standard error (eV)		0.337		0.152					
N		33		33					
slope (*m*)		0.2720		0.6399					
intercept (*b*)		0.366		0.714					
std error in *m*		0.0508		0.0396					
std error in *b*		0.059		0.033					

[a] All values in electronvolts. PMP2 calculations use spin annihilation and B3LYP/6-311G(d,p) geometries for anion and HF/6-31G(d) geometries for neutral. MP2/6-31+G(d,p) calculations for anion and HF/6-31G(d) geometries for neutral. MP2/6-31+G(d,p) calculations for species of 10 carbons and less are MP2-optimized except for cyclobutadiene, benzene, and indene. Data below the bold horizontal line are outliers and not included in the regressions. [b] The direct experimental gas-phase free energy is suspect, so the experimental value tabulated is estimated from reduction potential (vs Hg) and solvent effect with regression with 1/*r* (see Tables 1 and 2). [c] Calculated from CCSD(T) method; see text.

DFT theory with the two basis sets are very close to one another. In comparison with experiment, only the DFT data for 1,3-butadiene, cyclobutadiene, pentalene, **1**, and C_{60} are serious outliers, and they were excluded from the regression to avoid skewing the regression predictions. Indene, corannulene, and the pentalenes were also excluded because of questions about their experimental EAs and/or reduction potentials.

Regression errors are nearly identical for most molecules, within a few hundredths of an electronvolt, except for 1,3-butadiene, cyclobutadiene, and pentalene, where the regression errors at these two levels differ from one another by 0.14−0.22 eV. For C_{60}, the difference is a large 0.50 eV. Since this species has a much higher EA than the other PAHs, it might be less appropriate to use regression analysis to try to improve the reliability of the DFT calculations, though the predicted value from the regression is too negative by only 0.14 eV at the B3LYP/6-31+G(d,p) level. The absolute calculated value of $\Delta G^\circ_{a,298K}$ is very close to experiment at the B3LYP/6-311G(d,p) level but 0.49 eV too negative at the B3LYP/6-31+G(d,p) level.

Experimental EAs for the substituted pentalenes are estimated in a fashion similar to the cyclobutadienes and were excluded from the regression, even though agreement with theory is good. Indene's experimental EA is suspect, and no reliable literature

reduction potential could be found.[68] It was left out of the regression even though excellent agreement was obtained with an EA estimated from a peak reduction potential was measured by J. Parrish and R. D. Little here in DMF relative to that of naphthalene.

Less serious outliers are azulene, 1,1-diphenylethylene, and coronene, with DFT regression errors of about 0.1−0.2 eV. The B3LYP/6-31+G(d,p)-predicted $\Delta G°_{a,298K}$ for 1,1-diphenylethylene is 0.13 eV less negative than experiment, while the value predicted from the reduction potential is too negative by 0.06 eV. This is because we estimated the experimental value taking both these estimates into account. For coronene, both the quantum mechanical and reduction potential estimates suggest a slightly more negative EA, but the apparently reliable LPES experimental value seems preferable at this stage. These small regression errors appear to be near to the error limits of the experimental data, in terms of reproducibility and accuracy, substantiating the potential value of the theoretical results in making accurate predictions of relative energies for electron attachment and for pinpointing experimental results that might need to be reevaluated.

Both LPES and equilibrium data are available for azulene, anthracene, perylene, and cyclooctatetraene. The DFT-predicted free energy values agree well with both methods for anthracene and perylene. For azulene, the LPES negative free energy value (0.81 eV, Table 2) and the estimate from a solution reduction potential agree well with one another, but the DFT predictions (0.65 and 0.60 eV) are somewhat closer to the equilibrium free energy values of 0.67, 0.73, and 0.78 eV. For cyclooctatetraene, the DFT predictions (0.73 eV) are closer to the estimated negative free energy from LPES data (0.66 eV) than the equilibrium value (0.55 eV). The discrepancies between different values for azulene and cyclooctatetraene are somewhat larger than desirable and of unknown origin.

Between the correlations with solution reduction potentials, informed by predicted solvation energy effects in Table 2, and the correlations with DFT-calculated values in Table 5, we can see what appear to be some general patterns for experimental problems in the determination of gas-phase "electron affinities". As already reflected in our choice of the preferred experimental values in Table 1 and labeling of some experimental data there with question marks, there are many molecules with small positive EAs from ECD experiments where the EAs appear to be negative instead: naphthalene and the methylnaphthalenes, indene, styrene, biphenyl, and fluorene. The source of this problem may well be the same as for naphthalene, where the ECD experiments apparently lead to formation of negative ions that do not have the structure of the parent PAH anion. These ions are never identified directly in the ECD experiment. In the case of naphthalene, mass spectrometric experiments fail to reveal formation of the naphthalene radical anion under conditions that would normally lead to electron attachment if the EA were substantially positive.[23e,f] For these molecules, mass spectrometric experiments might clarify the interpretation of the ECD experiments. For 1,1-diphenylethylene and acenaphthylene, the experimental ECD EAs appear to be substantially different than those predicted by theory or solution data, as reflected in Tables 1, 2, and 5. In other cases, there is sometimes a scatter of ECD values of 0.2 eV but reasonably close agreement with the DFT predictions. In support of all of the reassignments in Table 1 is the fact that the theoretical predictions, in all cases, clearly favor the values reassigned on the basis of solution data in Tables 1 and 2.

For phenanthrene, a $-\Delta G°_{a,298K}$ value of 0.1 eV fits both the reduction potential data and DFT predictions better than the EA of 0.31 eV from ECD data, and some ECD values are as low as 0.20 eV. The EA of 0.7 eV for fluoranthene was chosen over the 0.63 eV value from ECD data because it better fits with the reduction potential and DFT predictions. For benzo[*c*]phenanthrene and dibenz[a,j]anthracene, approximate averages of various ECD values were chosen in Table 1 that better fit the regressions in Table 5 and the reduction potentials. For corannulene, the $-\Delta G°_{a,298K}$ predicted from its reduction potential is 0.8 eV, while the measured number from the apparently unreliable CID method is 0.50 eV. The predicted $-\Delta G°_{a,298K}$ from regression analysis from Table 5 is 0.79 eV, which is close to the assigned value from reduction potentials and far from the CID value.

The CID experiments on PAHs seem to be generally in error. The problem is most acute for biphenylene and C_{60} but is seen for benz[*a*]anthracene, benzo[ghi]perylene, corannulene, and perylene, as well. Only for anthracene, cyclooctatetraene, 1-methylanthracene, fluoranthene, pyrene, and coronene do the CID experiments seem to give the correct result. Again, the correlations with DFT-calculated results support this view. It is not clear why the CID kinetic method fails for electron transfer between PAH anions when it is so successful for many other reactions and for EAs of some substituted nitrobenzenes.[69]

For 1,3-butadiene and cyclobutadiene, the assigned EA values are based upon high-level theory and an ETS experiment for 1,3-butadiene. The two DFT results for 1,3-butadiene and cyclobutadiene differ from one another and are outliers by as much as 0.2 eV in Table 5. Since the CCSD(T) values for these two molecules in Table 4 differ significantly from the DFT results and agree with what is known experimentally, it appears that the DFT calculations, even with larger basis sets, do not describe the EAs of these two molecules as well as the others.

For pentalene, the agreement between the two DFT regressions is also large, and agreement with experiment is moderate. The "experimental" EA of 1.4 eV for pentalene was estimated in a fashion similar to that discussed above for cyclobutadiene on the basis of an experimental estimate for 1,3,5-tri-*tert*-butylpentalene from the Born model and calculated DFT EA differences in Table 5. This estimate fits the B3LYP/6-311G(d,p) predicted $\Delta G°_{a,298K}$ within 0.12 eV but differs from the B3LYP/6-31+G(d,p) prediction by 0.27 eV. The solvation analysis for tri-*tert*-butylpentalene gives an electron affinity from its reduction potential that fits the DFT calculated EA very well.[70] This might be surprising since the applicability of the Born model and solvation could be quite different from the PAHs. Though the charge delocalization in the conjugated aromatic rings differs in nature from that onto the alkyl groups attached to the pentalene anion, the Born model seems to fit both reasonably well.

Similarly, the dithia-substituted cyclobutadiene **1**, for which an experimental reduction potential is available, leads to a predicted $-\Delta G°_{a,298K}$ for **1** of 0.26 eV from eqs 2 and 4 in Table 2.[60] This value differs from the theoretically predicted $-\Delta G°_{a,298K}$ of 0.70 eV from Table 5 by more than usual. One question at issue in the electron-attachment reaction for **1** is whether the electron goes into an antibonding π orbital or whether it might be more localized on the sulfurs. Looking at orbital coefficients or electron and spin densities in the radical anion, we see that the DFT wave functions predict delocalization over both the π system and the two sulfur atoms. When we calculate the electron affinity of the CH_2 derivative **2** at the B3LYP/6-311G(d,p) level, we get a value 0.47 eV lower than for **1**, indicating that the

TABLE 7: Theoretical Koopmans' Theorem EAs and Experimental Free Energy for Electron Attachment[a]

	HF/ 6-311G(d,p) *E*(LUMO)	B3LYP/ 6-311G(d,p) *E*(LUMO)	B3LYP/ 6-31+G(d,p) *E*(LUMO)	HF/ 6-311G(d,p) *E*(HOMO,M$^-$)	B3LYP/ 6-311G(d,p) *E*(HOMO,M$^-$)	B3LYP/ 6-31+G(d,p) *E*(HOMO,M$^-$)	HF/ 6-311G(d,p) *E*(HOMO,M^{-*})	B3LYP/ 6-311G(d,p) *E*(HOMO,M^{-*})	ROVGF 6-311G(d,p) EA	$-\Delta G°_{a,298K}$
benzene	−3.71	0.26	0.42	−1.25	−3.59	−2.99	−1.80	−4.00	−2.61	−1.04
benzocyclobutadiene	−2.33	1.70	1.81	0.28	−1.69	−1.31	−0.59	−2.26		0.29
styrene	−2.79	1.15	1.28	−0.14	−2.20	−1.76	−1.00	−2.60		−0.1
azulene	−1.47	2.12	2.20	0.88	−1.19	−0.91	0.32	−1.49	−0.36	0.81
naphthalene	−2.55	1.26	1.33	−0.31	−2.09	−1.81	−0.92	−2.36	−1.55	−0.16
1-Menaphthalene	−2.56	1.22	1.29	−0.28	−2.01	−1.73	−0.92	−2.27		−0.2
2-Menaphthalene	−2.66	1.15	1.10	−0.29	−2.01	−1.77	−0.98	−2.37		−0.2
acenaphthylene	−1.48	2.16	2.22	0.87	−1.02	−0.79	0.13	−1.31		0.8
biphenylene	−2.30	1.51	1.58	−0.12	−1.51	−1.26	−0.76	−1.90	−1.09	0.2
biphenyl	−2.90	0.97	1.05	0.07	−1.76	−1.46	−1.16	−2.33		−0.1
fluorene	−2.66	1.02	1.10	−0.18	−1.94	−1.68	−0.88	−2.26		−0.1
anthracene	−1.69	1.91	1.96	0.50	−1.06	−0.88	−0.10	−1.26	−0.93	0.60
phenanthrene	−2.49	1.28	1.34	0.16	−1.63	−1.42	−0.54	−1.95		0.1
diphenylacetylene	−2.20	1.55	1.60	0.44	−1.15	−0.96	−0.36	−1.46		0.32
trans-stilbene	−2.19	1.65	1.73	0.75	−1.05	−0.84	−0.22	−1.40		0.35
1,1-diphenylethylene	−2.86	1.12	1.24	0.37	−1.45	−1.18	−0.83	−2.03		0.2
1-Meanthracene	−1.73	1.87	1.91	0.19	−1.03	−0.86	−0.13	−1.24		0.55
fluoranthene	−1.53	2.03	2.09	0.66	−0.81	−0.63	0.01	−1.08	0.22	0.7
pyrene	−1.81	1.75	1.80	0.42	−1.13	−0.96	−0.19	−1.35	−0.99	0.56
benz[*a*]anthracene	−1.75	1.83	1.87	0.39	−0.89	−0.74	−0.13	−1.09		0.70
benzo[*c*]phenanthrene	−2.01	1.60	1.64	0.27	−1.14	−0.99	−0.23	−1.33		0.40
chrysene	−2.12	1.54	1.58	0.22	−1.16	−1.00	−0.32	−1.38	−0.90	0.42
naphthacene	−1.10	2.35	2.38	1.07	−0.34	−0.21	0.53	−0.51	−0.01	1.02
triphenylene	−2.44	1.22	1.29	0.12	−1.46	−1.25	−0.47	−1.72	−1.18	0.29
benzo[*a*]pyrene	−1.50	2.00	2.04	0.83	−0.62	−0.49	0.31	−0.83	−0.34	0.77
benzo[*e*]pyrene	−1.86	1.67	1.73	0.39	−0.99	−0.82	−0.23	−1.19	−0.66	0.49
perylene	−1.28	2.17	2.24	0.90	−0.49	−0.31	0.33	−0.66	−0.53	1.00
benzo[ghi]perylene	−1.50	1.94	1.99	0.63	−0.66	−0.51	0.04	−0.84	−0.34	0.7
pentacene	−0.67	2.66	2.68	1.56	0.18	0.28	0.97	0.05		1.32
picene	−2.05	1.53	1.58	0.72	−0.90	−0.76	−0.07	−1.18	0.14	0.54
dibenz[a,h]anthracene	−1.80	1.76	1.80	0.31	−0.73	−0.60	−0.17	−0.93		0.68
dibenz[a,j]anthracene	−1.80	1.76	1.80	0.31	−0.76	−0.63	−0.20	−0.94		0.60
coronene	−1.74	1.68	1.71	0.41	−0.86	−0.75	−0.19	−1.04		0.57
cyclooctatetraene	−2.76	1.50	1.58	0.88	−0.69	−0.40	−1.39	−2.39		0.66
1,3-butadiene	−3.31	0.94	1.13	−0.42	−2.91	−2.21	−1.39	−3.50		−0.64
cyclobutadiene	−2.63	1.64	1.87	0.13	−2.24	−1.57	−0.72	−2.30		−0.08
pentalene	−1.13	2.79	2.88	0.73	−0.54	−0.19	0.34	−0.54		1.4
indene	−3.18	0.66	0.86	−0.42	−2.52	−2.19	−1.29	−3.08		−0.4
corannulene	−1.68	1.86	1.91	0.61	−0.84	−0.68	−0.44	−1.12		0.8
1		1.53	1.54		−0.37	−0.28				0.3
1,3,5-tri-*t*-Bu-pentalene		2.46	2.47		−0.03	0.05				1.3
1,3,5-triMepentalene		2.34	2.39		−0.51	−0.30				1.1
					regression statistics					
R^2	0.9300	0.9212	0.9141	0.8788	0.9323	0.9497	0.9449	0.9194	0.7807	
standard error (eV)	0.123	0.130	0.136	0.161	0.120	0.104	0.109	0.132	0.250	
N	33	33	33	33	33	33	33	33	15	
slope (*m*)	0.7166	0.9307	0.9608	0.8371	0.6415	0.7439	0.8024	0.5725	0.6279	
intercept (*b*)	1.862	−1.1092	−1.2159	0.114	1.196	1.162	0.658	1.272	0.926	
std error in *m*	0.0353	0.0489	0.0590	0.0558	0.0310	0.0307	0.0348	0.0305	0.0923	
std error in *b*	0.075	0.082	0.092	0.034	0.044	0.036	0.022	0.052	0.094	

[a] All values in electronvolts. Data below bold horizontal line not included in regressions.

unusually high EA for **1** is the result of electron delocalization onto the sulfur. The dioxa derivative **3** is predicted to have an EA a bit higher than for **1**, showing that the electronegativity of the heteroatom is a large factor in determining the stability of the radical anion. The small difference between predicted EAs of **2** and cyclobutadiene are consistent with the observation that alkyl substitution does not much affect the EAs of other PAHs in Table 5. The reduction potentials for **1** and **3** are predicted from their similar Born solvation energies and that for **2** about 0.4 eV more negative. The 0.4 eV discrepancy between the estimated experimental value and the predicted EAs for **1** might lie in either the experimental reduction potential or the theoretically calculated EA, or both. Perhaps the electron delocalization onto sulfur is somehow related to the problem.

The vertical negative electronic energy for electron attachment to C_{60} was calculated at the B3LYP/6-311G(d,p)//HF-6-31G(d) and B3LYP/6-31+G(d,p)//HF-6-31G(d) levels as 2.51 and 2.37 eV (2.18 and 2.09 from the regression equations), respectively, using the I_h geometry of the neutral hydrocarbon for the anion calculation. As discussed previously, the B3LYP/6-31+G(d,p) and B3LYP/6-311G(d,p) regression-predicted values at the B3LYP/6-311G(d,p) geometries for C_{60} and its anion (C_i symmetry) are 2.92 and 2.42 eV, respectively, agreeing only moderately well with the 2.78 eV value in Table 2. These results, however, clearly support the adiabatic EA from LPES measurements of 2.689 eV[63] and confirm that the CID value of 1.62 eV is anomalous.[25a] Zero-point and thermal energy corrections and entropy corrections were derived from our B3LYP/6-31G(d) frequency calculations on C_{60} and the C_i anion of C_{60}. The free energy for electron attachment in Table 2 for C_{70} is calculated from an LPES EA using thermodynamic corrections estimated from the calculated C_{60} values. Prior DFT

calculations on the C_{60} anion gave a D_{3d} geometry but without confirmatory frequency calculations.[71]

In Table 6 are shown data from MP2 calculations with the 6-31+G(d,p) basis set for those hydrocarbons where such calculations were convenient, and with the 6-31G(d) basis for the complete set. Also included are the results of the PMP2 spin annihilation methodology. The corrected EAs indeed usually give closer correlations with experiment in terms of absolute values and for the EA trends, which are evident in the regression data with experimental results summarized at the bottom of the table, as with Table 5. With the PMP2/6-31G(d) results the absolute values are seriously in error, and the standard error in the regression with experimental results is similar to the HF results in Table 5, at 0.15 eV. When regressions were carried out on the MP2 energies without spin annihilation, R^2 was only 0.267 and the standard error rose to 0.34 eV. At least part of the problem with the MP2 data can be seen from the spin-projection results. There are serious spin contamination problems noted earlier from the $<S^2>$ values at the HF level that are not completely removed for all molecules at the MP2 level, even after the PMP2 spin-annihilation correction (see Supporting Information). In fact, the spin annihilation procedure actually leads, counterintuitively, to increased values of $<S^2>$ in cases where the spin contamination is large. The reason for this is probably that there are significant contributions from very high spin states, sextets ($<S^2> = 8.75$) and octets ($<S^2> = 15.75$) in addition to quartet ($<S^2> = 3.75$) contamination. The PMP2 procedure removes only the quartet contamination, so that renormalization could well lead to an increase in $<S^2>$ as the fraction of these highest spin states increases.[72]

Table 7 shows the results of the Koopmans' Theorem methods for a large number of the aromatic hydrocarbons. Regression analysis results summarized at the bottom of Table 7 show standard errors of regression that range from 0.104 to 0.136 eV, except for the ROVGF method, which has much larger errors, with a standard error of 0.25 eV. The ROVGF method is known to perform better for low energy ionization energies than it does for electron affinities. This is a consequence of the approximation ROVGF uses to estimate the fourth- and higher-order terms. Better agreement might be obtained if UOVGF ionization energies were calculated for the radical anions, but these are very expensive calculations. In fact, with other Koopmans' Theorem results in Table 7, the best methods were based upon the energy of the HOMO of the radical anion, rather than the LUMO of the neutral hydrocarbon. These Koopmans' Theorem methods are useful, though not as reliable as the results in Table 5 using the ΔE method. The predicted $\Delta G^\circ_{a,298K}$ values from regressions with Koopmans' Theorem data generally agree well with those by the ΔE method and support the proposed reassignments of EAs.

Conclusions

We have found that a combination of theoretical calculations and experimental electron affinity and solution reduction potential data can be used to aid in the reinterpretation of the experimental data for PAHs to find a self-consistent interpretation of all the results. To accomplish this, we have tested the theoretical methods with a large enough set of experimental data to be able to conclude that $\Delta G^\circ_{a,298K}$ values can be predicted with reasonable reliability for PAHs and related hydrocarbons. Standard errors from linear regressions between theoretical and experimental free energies are 0.070 eV (mean unsigned error = 0.05 eV) and 0.077 eV for the ΔE method using density functional theory (DFT) methods, B3LYP/6-31+G(d,p) and B3LYP/6-311G(d,p), respectively. With the Hartree−Fock and MP2 methods, spin contamination is a problem, and larger standard errors of 0.13 to 0.15 eV are found, even with correction for the quartet spin state contamination by the PMP2 spin-projection methods. Koopmans' Theorem methods based upon HF and DFT LUMO(M) energies lead to standard errors of 0.12 to 0.14 eV, while those based upon HOMO($M^{-\bullet}$) energies give markedly smaller standard errors, as low as 0.10 eV for DFT methods with the radical anions. The OVGF Green's Function method gives a standard error of 0.25 eV.

Comparison of gas-phase free energies with solution-phase reduction potentials provides a measure of solvation energy differences between the radical anion and neutral PAH. A simple Born model approximates the dominant electrostatic solvation effects on the radical anions. This leads to a good correlation of experimental solvation energy differences with the inverse effective ionic radius, assuming that the PAH anions may be approximated as spheres with the same volumes as those derived from DFT electron-density envelopes of the PAH anions. This implementation of the Born model leads to a very useful procedure for the estimation of unknown or questionable $\Delta G^\circ_{a,298K}$ values from experimental reduction potentials. Such a procedure is a general one that could be applied to other molecules and to thermodynamic data for other gas- and solution-phase reactions, such as ionization to radical cations (ionization potentials) and protonation (gas-phase basicities). This sort of theoretical approach can be extended to ions not well described as approximate spheres of nearly even charge distribution by using the generalized Born theory incorporated into current theoretical models for solvation.[55] We are currently pursuing such studies.

The Born model has been used to relate the electrostatic solvation energies of PAH and hydrocarbon radical anions and spherical halide anions, and alkali metal cations, and ammonium ions to effective ionic radii from DFT electron-density envelopes. Standard errors in regressions based upon the Born model are as low as 2−3 kcal mol^{-1}, which is the same magnitude as the standard errors in prediction of $\Delta G^\circ_{a,298K}$ values from DFT calculations and the variability of some experimental EA and reduction potential data (ca. 0.1 eV). A free energy of solvation term has been derived from experimental $\Delta G^\circ_{a,298K}$ and reduction potential data for the very large spherical radical anion from C_{60}. The Born model used for PAHs has been successfully extended here to quantitatively explain the solvation energy of the C_{60} and C_{70} radical anions.

The two independent estimates of $\Delta G^\circ_{a,298K}$ values from reduction potentials and Born theory and from the ab initio and DFT calculations lead us to propose reassignments for nearly one-half (17 of 38) of the PAHs and related molecules for which experimental EAs have been reported: styrene, indene, biphenylene, biphenyl, fluorene, phenanthrene, the methylnaphthalenes, acenaphthylene, 1,1-diphenylethylene, fluoranthene, corannulene, perylene, benzo[ghi]perylene, benz[*a*]anthracene, benzo[*c*]phenanthrene, dibenz[a,j]anthracene, and perhaps coronene. DFT calculation of the electron affinity for C_{60} is consistent with the LPES measurement and confirms that the CID measurement does not properly determine the adiabatic electron affinity. The prevalence of such discrepancies, sometimes large, between EAs of PAHs measured by the CID method and other methods or predicted from both our DFT calculations and estimates from solution reduction potentials and the Born model suggests that there may be a systematic problem with the interpretation of these experiments. The concept of a "local" electron affinity for C_{60} has been proposed in this context.[25a]

Our conclusion that the problems with application of the CID method to EAs of PAHs are widespread suggests that further experimental work would be in order to help define the scope of the problem and the fundamental origin of the peculiar kinetic effects that must be operating. We explored the possibility that these anomalies might be related to the possible formation of a covalently bound anion−neutral σ complex in the CID experiments by calculating the geometries and energies of π and σ complexes for anthracene and its anion. Surprisingly, the free energy for formation of the π complex was favorable by 0.11 eV and unfavorable by 1.29 eV for the σ complex, calling into question the notion that σ complex formation might explain the CID anomalies.

The dithia-substituted cyclobutadiene **1** reveals an anomalous reduction potential and EA due to electron delocalization onto the sulfurs. This is confirmed by comparing its calculated EA with those for derivatives **2** and **3** lacking the sulfur. For **1**, there is a significant discrepancy (0.4 eV) when the theoretically predicted EA and estimated EA from the experimental reduction potential are compared, but the estimation of the EA for cyclobutadiene from the reduction potential of **1** leads to a value consistent with that from high-level quantum theory (−0.08 eV) and to an estimated reduction potential (1.6 eV vs Hg). Similarly, with the aid of the Born model, the experimental reduction potential for the antiaromatic hydrocarbon, 1,3,5-tri-*tert*-butylpentalene, leads to an estimated EA (1.3 eV) that is close to that expected from DFT calculations. This combination of experimental and theoretical methods also provides a basis for the estimation of both the reduction potential (0.4 eV vs Hg) and EA (1.4 eV) of pentalene with some degree of confidence and suggests that this methodology could be extended to the predictions for many other molecules for which either or both of these experimental quantities are not available.

Acknowledgment. We acknowledge the use of the National Environmental Supercomputing Center (NESC2) and associated support. We thank John Parrish and R. D. Little for carrying out cyclic voltammetry measurements on indene, and V. G. Zakrzewski for useful discussions and help with the OVGF calculations. We also thank Dr. Douglas Dudis at Wright-Patterson Air Force Base for sharing DFT data on C_{60} and its anion. The U. S. EPA, through its Office of Research and Development, funded and performed the research described. This paper has been subjected to the EPA's peer and administrative review and has been approved for publication. Mention of trade names or commercial products does not constitute endorsement or recommendation by EPA for use.

Supporting Information Available: Tables S1−S3 with raw electronic energies and thermochemical data. Table S4 with ionic states' symmetries and spin-projection data. Table S5 with regression errors from Koopmans' Theorem analysis and ionic geometry-relaxation energies upon ionization. Table S6 with HF/6-311G(d,p) and B3LYP/6-311G(d,p) geometries. This material is available free of charge via the Internet at http://pubs.acs.org.

References and Notes

(1) (a) Clar, E. *Polycyclic Hydrocarbons*; Academic Press: London, 1964; Vols. 1, 2. (b) Gutman, I., Cyvin, S. J., Eds. *Topics in Current Chemistry: Advances in the Theory of Benzenoid Hydrocarbons*; Springer-Verlag: New York, 1990; Vol. 153.

(2) Streitwieser, A., Jr. *Molecular Orbital Theory for Organic Chemists*; Wiley: New York, 1961.

(3) (a) Grimmer, G. *Environmental Carcinogens: Polycyclic Aromatic Hydrocarbons;* CRC Press: Boca Raton, FL, 1983. (b) *Polycyclic Aromatic Hydrocarbon Carcinogenesis: Structure−Activity Relationships*; CRC Press: Boca Raton, FL, 1988. (c) Harvey, R. G. *Polycyclic Aromatic Hydrocarbons: Chemistry and Carcinogenesis*; Cambridge University Press: Cambridge, 1991.

(4) (a) Yürüm, Y., Ed. *New Trends in Coal Science*, NATO ASI Series C: Mathematical and Physical Sciences 244; Kluwer Academic Publishers: Dordrecht, The Netherlands, 1988. (b) Harris, S. J.; Weiner, A. M. *Combust. Sci. Technol*. **1983**, *51*, 265. (c) Frenklach, M.; Warnatz, J. *Combust. Sci. Technol*. **1997**, *31*, 155. (d) Finlayson-Pitts, B. J.; Pitts, J. N., Jr. *Science* **1997**, *276*, 1045.

(5) (a) *Sampling and Analysis Methods for Hazardous Waste Combustion—Methods 3500, 3540, 3610,* 3630, *8100, 8270, and 8310; Test Methods for Evaluating Solid Waste (SW-846)*; U. S. Environmental Protection Agency, Office of Solid Waste: Washington, D. C. (b) *Measurement of Polycyclic Organic Matter for Environmental Assessment*; U. S. Environmental Protection Agency, Industrial Environmental Research Laboratory: Research Triangle Park, NC, EPA-600/7-79-191, August 1979. (c) Riggin, R. M. *Compendium of Methods for the Determination of Toxic Organic Compounds in Ambient Air*; U. S. Environmental Protection Agency, EMSL, Quality Assurance Division: Research Triangle Park, NC, EPA-600/4-84-041, April 1984.

(6) (a) Sanford, S. A. *Fundam. Cosmic Phys.* **1987**, *12*, 1. (b) Allamandola, L. J.; Sanford, S. A.; Wopenka, B. *Science* **1987**, *237*, 56. (c) Clemett, S.; Marchling, C.; Zare, R. N.; Swan, P.; Walker, R. *Science* **1993**, *262*, 721. (d) Le Page, V.; Keheyan, Y.; Snow, T. P.; Bierbaum, V. M. *Int. J. Mass Spectrom*. **1999**, *187*, 949. (e) Snow, T. P.; Le Page, V.; Keheyan, Y.; V. M. Bierbaum, V. M. *Nature* **1998**, *391*, 259. (f) Henning, T.; Salama, F. *Science* **1998**, *282*, 2204. (g) Sloan, G. C.; Hayward, T. L.; Allamandola, L. J.; Bregman, J. D.; DeVito, B.; Hudgins, D. M. *Astrophys. J*. **1999**, *513*, L65. (h) Ehrenfreund, P. *Science* **1999**, *283*, 1123. (i) Bernstein, M. P.; Sanford, S. A.; Allamandola, L. J.; Gillette, J. S.; Clement, S. J.; Zare, R. N. *Science* **1999**, *283*, 1135. (j) Hellemans, A. *Science* **2000**, *287*, 946.

(7) (a) Bakes, E. L. O.; Tielens, A. G. G. M. *Astrophys. J.* **1998**, *499*, 258. (b) Szczepanski, J.; Wehlburg, C.; Vala, M. *Chem. Phys. Lett.* **1995**, *232*, 221. (c) Langhoff, S. R. *J. Phys. Chem.* **1996**, *100*, 2819. (d) Hudgins, D. M.; Bauschlicher, C. W.; Allamandola, L. J.; Fetzer, J. C. *J. Phys. Chem. A* **2000**, *104*, 3655. (e) Halsinski, T. M.; Hudgins, D. M.; Salama, F.; Allamandola, L. J.; Bally, T. *J. Phys. Chem. A* **2000**, *104*, 7484.

(8) (a) Brouwer, A. C.; Groenen, E. J. J.; van Hemert, M. C.; Schmidt, J. *J. Phys. Chem. A* **1999**, *103*, 8959. (b) Guo, X.; Grützmacher, H. F. *J. Am. Chem. Soc.* **1999**, *121*, 4485.

(9) (a) Martin, J. M. L.; El-Yazal, J.; François, J. P. *Chem. Phys. Lett.* **1996**, *248*, 345 and references therein. (b) Martin, J. M. L. *Chem. Phys. Lett.* **1996**, *262*, 97.

(10) (a) *Fullerenes Synthesis, Properties, and Chemistry of Large Carbon Clusters*; Hammond, G., Kuck, V. J., Eds.; ACS Symposium Series 481; American Chemical Society: Washington, DC, 1992. (b) Diederich, F.; Isaacs, L.; Philp, D. *Chem. Soc Rev.* **1994**, 243. (c) Hirsch, A. *The Chemistry of Fullerenes*; Thieme: Stuttgart, 1994. (d) Diederich, F.; Thilgen, C. *Science* **1996**, *271*, 317. (e) Hirsch, A. *Top. Curr. Chem*. **1999**, *199*, 1. (f) Thilgen, C.; Diederich, F. *Top. Curr. Chem*. **1999**, *199*, 135.

(11) (a) Gonzalez, C.; Lim, E. C. *J. Phys. Chem. A* **2000**, *104*, 2953. (b) Schön, J. H.; Kloc, C.; Batlogg, B. *Science* **2000**, *288*, 2338.

(12) (a) *Handbook of Polycyclic Aromatic Hydrocarbons*; Bjørseth, A., Ed.; Marcel Dekker: New York, 1983; Vol. 1. (b) Neilson, A. H., Ed. *The Handbook of Environmental Chemistry: PAHs and Related Compounds*; Springer-Verlag: New York, 1998; Vol. 3, Part 1.

(13) Lee, M. L.; Novotny, M. V.; Bartle, K. D. *Analytical Chemistry of Polyaromatic Hydrocarbons*; Academic Press: New York, 1981.

(14) Berry, K. A. T.; Burton, D. L. *Can. J. Soil Sci*. **1997**, *77*, 469.

(15) (a) Pointet, K.; Milliet, A.; Hoyau, S.; Renou-Gonnord, M. F. *J. Comput. Chem*. **1997**, *18*, 629. (b) Pointet, K.; Milliet, A.; Renou-Gonnord, M. F. *J. Mass Spectrom*. **1995**, *30*, 1495. (c) See also: Hand, O. W.; Winger, B. E.; Cooks, R. G. *Biomed. Environ. Mass Spectrom*. **1989**, *16*, 83.

(16) Aue, D. H.; Guidoni, M.; Betowski, L. D. *Int. J. Mass Spectrom.* **2000**, *201*, 283.

(17) (a) Betowski, L. D.; Webb, H. M.; Sauter, A. D. *Biomed. Mass Spectrom*. **1983**, *10*, 369. (b) Betowski, L. D.; Enlow, M.; Aue, D. H. *Int. J. Mass Spectrom.* **2006**, *255−256*, 123.

(18) (a) Daishima, S.; Iida, Y.; Shibata, A.; Kanda, F. *Org. Mass Spectrom*. **1992**, *27*, 571. (b) Buchanan, M. V.; Olerich, G. *Org. Mass Spectrom*. **1984**, *19*, 486. (c) Oehme, M. *Anal. Chem*. **1983**, *55*, 2290. (d) Hilpert, L. R.; Byrd, G. D.; Vogt, C. R. *Anal. Chem*. **1984**, *56*, 1842. (e) Low, G. K.-C.; Batley, G. E.; Lidgard, R. O.; Duffield, A. M. *Biomed. Environ. Mass Spectrom*. **1986**, *13*, 95. (f) Grimsrud, E. P. *Anal. Chem*. **1984**, *56*, 1797.

(19) EAs have recently been calculated using six DFT methods for the first four linear PAHs: (a) Rienstra-Kiracofe, J. C.; Barden, C. J.; Brown, S. T.; Schaefer, H. F. *J. Phys. Chem. A* **2001**, *105*, 524. See also: (b) Gonzales, J. M.; Barden, C. J.; Brown, S. T.; Schleyer, P. v. R.; Schaefer, H. F.; Li, Q.-S. *J. Am. Chem. Soc*. **2003**, *125*, 1064. (c) Rienstra-Kiracofe,

J. C.; Tschumper, G. S.; Schaefer, H. F.; Nandi, S.; Ellison, G. B. *Chem. Rev*. **2002**, *102*, 231.

(20) NIST *Standard Reference Database Number 69*, March 1998 Release, Negative Ion Energetics data compiled by Bartmess, J. E. (http://webbook.nist.gov/chemistry/).

(21) (a) Wentworth, W. E.; Becker, R. S. *J. Am. Chem. Soc*. **1962**, *84*, 4263. (b) Becker, R. S.; Chen, E. *J. Chem. Phys.* **1966**, *45*, 2403. Common-intercept method: (c) Lyons, L. E.; Morris, G. C.; Warren, L. J. *J. Phys. Chem.* **1968**, *72*, 3677. (d) Michl, J. *J. Mol. Spectrosc*. **1969**, *30*, 66. (e) Wentworth, W. E.; Ristau, W. *J. Phys. Chem*. **1969**, *73*, 2126. (f) Wojnárovits, L.; Földiák, G. *J. Chromatogr*. **1981**, *206*, 511. Determined-intercept method: (g) Zlatkis, A.; Lee, C. K.; Wentworth, W. E.; Chen, E. C. M. *Anal. Chem*. **1983**, *55*, 1596. (h) Chen, E. C. M.; Chen, E. S.; Milligan, M. S.; Wentworth, W. E.; Wiley, J. R. *J. Phys. Chem.* **1992**, *96*, 2385. (i) Ruoff, R. S.; Kadish, K. M.; Boulas, P.; Chen, E. C. M. *J. Phys. Chem*. **1995**, *99*, 8843. Determined-intercept method: (j) Wiley, J. R.; Chen, E. C. M.; Wentworth, W. E. *J. Phys. Chem*. **1993**, *97*, 1256. (k) Chen, E. C.; Wentworth, W. E. *J. Chem. Phys.* **1975**, *63*, 3183 and references therein.

(22) Chaney, E. L.; Christophorou, L. G.; Collins, P. M.; Carter, J. C. *J. Chem. Phys*. **1970**, *52*, 4413.

(23) (a) Grimsrud, E. P.; Chowdhury, S.; Kebarle, P. *J. Chem. Phys*. **1985**, *83*, 3983. (b) Kato, S.; Lee, H. S.; Gareyev, R.; Wenthold, P. G.; Lineberger, W. C.; DePuy, C. H.; Bierbaum, V. M. *J. Am. Chem. Soc*. **1997**, *119*, 7863. (c) Chowdhury, S.; Heinis, T.; Grimsrud, E. P.; Kebarle, P. *J. Phys. Chem*. **1986**, *90*, 2747. (d) Kebarle, P.; Chowdhury, S. *Chem. Rev*. **1987**, *87*, 513. (e) Heinis, T.; Chowdhury, S.; Kebarle, P. *Org. Mass Spectrom*. **1993**, *28*, 358. (f) Crocker, L.; Wang, T. B.; Kebarle, P. *J. Am. Chem. Soc.* **1993**, *115*, 7818. (g) Chowdhury, S.; Heinis, T.; Kebarle, P. *J. Am. Chem. Soc*. **1986**, *108*, 4662.

(24) Broadus, K. M.; Kass, S. R. *J. Am. Chem. Soc*. **2000**, *122*, 10697.

(25) (a) Chen, G.; Cooks, R. G.; Corpuz, E.; Scott, L. T. *J. Am. Soc. Mass Spectrom*. **1996**, *7*, 619. (b) Chen, G. D.; Cooks, R. G. *J. Mass Spectrom*. **1995**, *30*, 1167. (c) Deault, J. W.; Chen, G.; Cooks, R. G. *J. Am. Soc. Mass Spectrom*. **1998**, *9*, 1141.

(26) (a) Staley, S. W.; Strnad, J. T. *J. Phys. Chem*. **1994**, *98*, 116. (b) Burrow, P. D.; Michejda, J. A.; Jordan, K. D. *J. Chem. Phys.* **1987**, *86*, 9.

(27) (a) Gygax, R.; McPeters, H. L.; Brauman, J. I. *J. Am. Chem. Soc.* **1979**, *101*, 2567. (b) Wenthold, P. G.; Hrovat, D. A.; Borden, W. T.; Linebeger, W. C. *Science* **1996**, *272*, 1456. (c) Schiedt, J.; Weinkauf, R. *Chem. Phys. Lett.* **1997**, *266*, 201. (d) Schiedt, J.; Weinkauf, R. *Chem. Phys. Lett*. **1997**, *274*, 18. (e) Schiedt, J.; Knott, W. J.; Le Barbu, K.; Schlag, E. W.; Weinkauf, R. *J. Chem. Phys.* **2000**, *113*, 9470. (f) Lyapustina, S. A.; Xu, S.; Nilles, J. M.; Bowen, K. H. *J. Chem. Phys.* **2002**, *116*, 4477. (g) Song, J. K.; Han, S. Y.; Chu, I. H.; Kim, J. H.; Kim, S. K.; Lyapustina, S. A.; Xu, S.; Nilles, J. M.; Bowen, K. H. *J. Chem. Phys.* **2000**, *112*, 6643. (h) Duncan, M. A.; Knight, A. M.; Negishi, Y.; Nagao, S.; Nakamura, Y.; Kato, A.; Nakajima, A.; Kaya, K. *Chem. Phys. Lett*. **1999**, *309*, 49. (i) Nimlos, M. R.; Ellison, B. G. *J. Chem. Phys.* **2000**, *90*, 2574.

(28) (a) Koopmans, T. *Physica* **1933**, *1*, 104. (b) For the use Koopmans' Theorem with DFT theory see: Stowasser, R.; Hoffman, R. *J. Am. Chem. Soc*. **1999**, *121*, 3414.

(29) von Niessen, W.; Schirmer, J.; Cederbaum, L. S. *Comput. Phys. Rep*. **1984**, *1*, 57.

(30) Notario, R.; Abboud, J. L. M. *J. Phys. Chem. A* **1998**, *102*, 5290.

(31) Ellinger, Y.; Pauzat, F.; Lengsfield, B. H. *J. Mol. Struct. (THEOCHEM)* **1999**, *458*, 203.

(32) Torii, H. J. *J. Phys. Chem. A* **2000**, *104*, 413.

(33) Halasinski, T. M.; Hudgins, D. M.; Salama, F.; Allamandola, L. J.; Bally, T. J. *J. Phys. Chem. A* **2000**, *104*, 7484.

(34) Bauschlicher, C. W.; Hudgins, D. M.; Allamandola, L. J. *Theor. Chem. Acc.* **1999**, *103*, 154.

(35) Tschumper, G. S.; Schaefer, H. F., III. *J. Chem. Phys.* **1997**, *106*, 2529.

(36) Rienstra-Kiracofe, J. C.; Graham, D. E.; Schaefer, H. F., III. *Mol. Phys*. **1998**, *94*, 767.

(37) Brown, S. T.; Rienstra-Kiracofe, J. C.; Schaefer, H. F., III. *J. Phys. Chem. A* **1999**, *103*, 4065.

(38) Brown, S. T.; Rienstra-Kiracofe, J. C.; Schaefer, H. F., III. *J. Phys. Chem. A* **1999**, *103*, 4129.

(39) (a) Zakrzewski, V. G.; Ortiz, J. V. *Int. J. Quantum Chem., Quantum Chem. Symp*. **1994**, *28*, 23. (b) Zakrzewski, V. G.; Ortiz, J. V. *Int. J. Quantum Chem.* **1995**, *53*, 583.

(40) (a) Frisch, M. J.; Trucks, G. W.; Schlegel, H. B.; Gill, P. M. W.; Johnson, B. G.; Robb, M. A.; Cheeseman, J. R.; Keith, T.; Petersson, G. A.; Montgomery, J. A.; Raghavachari, K.; Al-Laham, M. A.; Zakrzewski, V. G.; Ortiz, J. V.; Foresman, J. B.; Cioslowski, J.; Stefanov, B. B.; Nanayakkara, A.; Challacombe, M.; Peng, C. Y.; Ayala, P. Y.; Chen, W.; Wong, M. W.; Andres, J. L.; Replogle, E. S.; Gomperts, R.; Martin, R. L.; Fox, D. J.; Binkley, J. S.; Defrees, D. J.; Baker, J.; Stewart, J. P.; Head-Gordon, M.; Gonzalez, C.; Pople, J. A. *Gaussian 94*, revision E.2; Gaussian, Inc.: Pittsburgh, PA, 1995. (b) Frisch, M. J.; Trucks, G. W.; Schlegel, H. B.; Scuseria, G. E.; Robb, M. A.; Cheeseman, J. R.; Zakrzewski, V. G.; Montgomery, J. A., Jr.; Stratmann, R. E.; Burant, J. C.; Dapprich, S.; Millam, J. M.; Daniels, A. D.; Kudin, K. N.; Strain, M. C.; Farkas, O.; Tomasi, J.; Barone, V.; Cossi, M.; Cammi, R.; Mennucci, B.; Pomelli, C.; Adamo, C.; Clifford, S.; Ochterski, J.; Petersson, G. A.; Ayala, P. Y.; Cui, Q.; Morokuma, K.; Malick, D. K.; Rabuck, A. D.; Raghavachari, K.; Foresman, J. B.; Cioslowski, J.; Ortiz, J. V.; Stefanov, B. B.; Liu, G.; Liashenko, A.; Piskorz, P.; Komaromi, I.; Gomperts, R.; Martin, R. L.; Fox, D. J.; Keith, T.; Al-Laham, M. A.; Peng, C. Y.; Nanayakkara, A.; Gonzalez, C.; Challacombe, M.; Gill, P. M. W.; Johnson, B. G.; Chen, W.; Wong, M. W.; Andres, J. L.; Head-Gordon, M.; Replogle, E. S.; Pople, J. A. *Gaussian 98*, revision A.6; *Gaussian 98*, revision A.2; Gaussian, Inc.: Pittsburgh, PA, 1998. (c) Frisch, M. J.; Trucks, G. W.; Schlegel, H. B.; Scuseria, G. E.; Robb, M. A.; Cheeseman, J. R.; Montgomery, J. A., Jr.; Vreven, T.; Kudin, K. N.; Burant, J. C.; Millam, J. M.; Iyengar, S. S.; Tomasi, J.; Barone, V.; Mennucci, B.; Cossi, M.; Scalmani, G.; Rega, N.; Petersson, G. A.; Nakatsuji, H.; Hada, M.; Ehara, M.; Toyota, K.; Fukuda, R.; Hasegawa, J.; Ishida, M.; Nakajima, T.; Honda, Y.; Kitao, O.; Nakai, H.; Klene, M.; Li, X.; Knox, J. E.; Hratchian, H. P.; Cross, J. B.; Bakken, V.; Adamo, C.; Jaramillo, J.; Gomperts, R.; Stratmann, R. E.; Yazyev, O.; Austin, A. J.; Cammi, R.; Pomelli, C.; Ochterski, J. W.; Ayala, P. Y.; Morokuma, K.; Voth, G. A.; Salvador, P.; Dannenberg, J. J.; Zakrzewski, V. G.; Dapprich, S.; Daniels, A. D.; Strain, M. C.; Farkas, O.; Malick, D. K.; Rabuck, A. D.; Raghavachari, K.; Foresman, J. B.; Ortiz, J. V.; Cui, Q.; Baboul, A. G.; Clifford, S.; Cioslowski, J.; Stefanov, B. B.; Liu, G.; Liashenko, A.; Piskorz, P.; Komaromi, I.; Martin, R. L.; Fox, D. J.; Keith, T.; Al-Laham, M. A.; Peng, C. Y.; Nanayakkara, A.; Challacombe, M.; Gill, P. M. W.; Johnson, B.; Chen, W.; Wong, M. W.; Gonzalez, C.; Pople, J. A. *Gaussian 03*, revision B.05; Gaussian, Inc.: Wallingford, CT, 2004.

(41) Gill, P. M. W. In *Encyclopedia of Computational Chemistry*; Schleyer, P. v. R., Ed.; John Wiley: New York, 1998; Vol. 1, p 678.

(42) Becke, A. D. *J. Chem. Phys*. **1993**, *98*, 5648.

(43) (a) Cremer, D. In *Encyclopedia of Computational Chemistry*; Schleyer, P. v. R., Ed.; John Wiley: New York, 1998; Vol. 2, p 1706. (b) Hehre, W. J.; Radom, L.; Schleyer, P. v. R.; Pople, J. A. *Ab Initio Molecular Orbital Theory*; John Wiley and Sons: New York, 1986; p 38.

(44) Gauss, J. In *Encyclopedia of Computational Chemistry*; Schleyer, P. v. R., Ed.; John Wiley: New York, 1998; Vol. 1, p 615.

(45) Del Bene, J. E.; Aue, D. H.; Shavitt, I. *J. Am. Chem. Soc.* **1992**, *114*, 1631.

(46) See ref 43b, p 76.

(47) Dunning, T. H., Jr.; Peterson, K. A. In *Encyclopedia of Computational Chemistry*; Schleyer, P. v. R., Ed.; John Wiley: New York, 1998; Vol. 1, p 88.

(48) (a) Aue, D. H. In *Encyclopedia of Computational Chemistry*; Schleyer, P. v. R., Ed.; John Wiley: New York, 1998; Vol. 1, p 210. (b) Aue, D. H. In *Dicoordinated Carbocations*; Rappoport, Z., Stang, P. J., Eds.; John Wiley: Chichester, U.K., 1997; pp 105−157.

(49) (a) Schlegel, H. B. *J. Phys. Chem. A* **1999**, *103*, 4065. (b) Schlegel, H. B. In *Encyclopedia of Computational Chemistry*; Schleyer, P. v. R., Ed.; John Wiley: New York, 1998; Vol. 4, p 2665.

(50) (a) Scott, A. P.; Radom, L. *J. Phys. Chem.* **1996**, *100*, 16502. (b) Aue, D. H.; Caras, J.; Guidoni, M. To be published. We have evaluated optimium scale factors for numerous PAHs and their anions and find that the DFT scale factors differ with basis set between 0.96 for the B3LYP/4-31G or 6-31G(d) levels to 0.97 for the B3LYP/6-311G(d,p) level. For thermal terms and entropies, such variation has little effect. For zero-point energies, the 0.99 scale factor fits experimental zero-point energies for unsaturated hydrocarbons reasonably well.

(51) (a) Mann, C. K.; Barnes, K. K. *Electrochemical Reactions in Nonaqueous Systems*; Marcel Dekker: New York, 1970. (b) Fry, A. J.; Fox, P. C. *Tetrahedron* **1986**, *42*, 5255. (c) Streitweiser, A., Jr.; Schwager, I. *J. Phys. Chem*. **1962**, *66*, 2316. (d) Seiders, T. J.; Baldridge, K. K.; Siegel, J. S.; Gleiter, R. *Tetrahedron Let*. **2000**, 4519. (e) Pappin, A. J.; Tytko, A. P.; Bartle, K. D.; Taylor, N.; Mills, D. G. *Fuel* **1987**, *66*, 1050.

(52) (a) Grimsrud, E. P.; Caldwell, G.; Chowdhury, S.; Kebarle, P. *J. Am. Chem. Soc*. **1985**, *107*, 4627. (b) Heinis, T.; Chowdhury, S.; Scott, S. L.; Kebarle, P. *J. Am. Chem. Soc*. **1988**, *110*, 400. (c) Kebarle, P. *J. Am. Chem. Soc.* **1989**, *111*, 464.

(53) (a) Winget, P.; Weber, E. J.; Cramer, C. J.; Truhlar, D. G. *Phys. Chem. Chem. Phys.* **2000**, *2*, 1231. (b) Winget, P.; Cramer, C. J.; Truhlar, D. G. *Theor. Chem. Acc.* **2004**, *112*, 217. (c) Lewis, A.; Bumpus, J. A.; Cramer, C. J.; Truhlar, D. G. *J. Chem. Educ*. **2004**, *81*, 596. (d) Rienstra-Kiracofe, J. C.; Tschumper, D. E.; Schaefer, H. F., III; Nandi, S.; Ellison, G. B. *Chem. Rev.* **2002**, *102*, 231.

(54) (a) Wauchope, R. D.; Haque, R. *Can. J. Chem*. **1972**, *50*, 133. (b) Acree, W. E., Jr.; Abraham, M. H. *Fluid Phase Equilib*. **2002**, *201*, 245. (c) Acree, W. E., Jr.; Abraham, M. H. *Can. J. Chem*. **2001**, *79*, 1466. (d) Marcus, Y.; Smith, A. L.; Korobov, M. V.; Mirakyan, A. L.; Avramenko, N. V.; Stukalin, E. B. *J. Phys. Chem. B* **2001**, *105*, 2499. (e) Marcus, Y.; Smith, A. L.; Korobov, M. V.; Mirakyan, A. L.; Avramenko, N. V.; Stukalin, E. B.; Olofsson, G.; Smith, A. L.; Ruoff, R. S. *J. Phys. Chem. B* **1999**, *103*, 2499.

(55) (a) Kim, K. S.; Lee, J. Y.; Choi, H. S.; Kim, J.; Jang, J. H. *Chem. Phys. Lett*. **1997**, *265*, 497. (b) Sandberg, L.; Casemyr, R.; Edholm, O. *J.*

Chem. Phys. **2002**, *106*, 7889. (c) Chambers, C. C.; Hawkins, G. D.; Cramer, C. J.; Truhlar, D. G. *J. Chem. Phys*. **1996**, *100*, 16385. (d) Cramer, C. J.; Truhlar, D. G. *Chem. Rev*. **1999**, *99*, 2161.

(56) For example, benzene, toluene, ethylbenzene, 2-propylbenzene, naphthalene, biphenyl, phenanthrene, anthracene, and pyrene have free energies of hydration of −0.87, −0.89, −0.80, −0.31, −2.39, −2.63, −3.95, −4.23, and −4.57 kcal mol^{-1}, respectively; see ref 55b.

(57) Raimondi, M.; Calderoni, G.; Raimondi, L.; Cozzi, F. *J. Phys. Chem. A* **2003**, *107*, 772; *J. Chem. Phys.* **2002**, *106*, 7889 and references therein.

(58) Aue, D. H.; Webb, H. M.; Bowers, M. T. *J. Am. Chem. Soc*. **1976**, *98*, 318.

(59) (a) Hopkins, H. P., Jr.; Jahagirdar, D. V.; Moulik, S. P.; Aue, D. H.; Webb, H. M.; Davidson, W. R.; Pedley, M. D. *J. Am. Chem. Soc*. **1984**, *106*, 1770. (b) Aue, D. H.; Webb, H. M.; Davidson, W. R.; Toure, P.; Hopkins, H. P., Jr.; Moulik, S. P.; Jahagirdar, D. V. *J. Am. Chem. Soc.* **1991**, *113*, 1770.

(60) Born, M. *Phys. Z.* **1920**, *1*, 45.

(61) This Born solvation theory approach was suggested for PAHs before there were sufficient experimental data to test it. Matsen, F. A. *J. Chem. Phys.* **1955**, *24*, 602.

(62) . (a) Latimer, W. M.; Pitzer, K. S.; Slansky, C. M. *J. Chem. Phys.* **1939**, *7*, 108. (b) Gouray, B. S.; Adrian, F. *J. Solid State Phys.* **1960**, *10*, 127. (c) Blandamer, M. J.; Symons, M. C. R. *J. Phys. Chem.* **1963**, *67*, 1304. (d) Noyes, R. M. *J. Am. Chem. Soc*. **1962**, *84*, 513. (e) Muirhead-Gould, J. S.; Laidler, K. J. *Trans. Faraday Soc.* **1967**, *63*, 944. (f) Burgess, J. *Metal Ions in Solution*; Ellis Harwood: Chichester, U.K., 1978. (g) Bockris, J. O.; Reddy, A. K. N. *Modern Electrochemistry*; Plenum Press: New York, 1977; Vol. 1, Chapter 2. (h) Friedman, H.: Krishnan, C. V. In *Water, A Comprehensive Treatise*; Franks, F. F., Ed.; Plenum Press: New York, 1973; Vol. 3, Chapter 1. (i) Rashin, A. A.; Honig, B. *J. Phys. Chem.* **1985**, *89*, 5588. (j) Marcus, Y. *Chem. Rev*. **1988**, *88*, 1475. (k) Boyd, R. H. *J. Chem. Phys.* **1969**, *51*, 1470. (l) Nagano, Y.; Sakiyama, M.; Fujiwara, T.; Kondo, Y. *J. Phys. Chem.* **1988**, *92*, 5823. (m) Bucher, M. *J. Phys. Chem.* **1991**, *95*, 663. (n) Babu, C. S.; Lim, C. *J. Phys. Chem. B* **1999**, *103*, 7958. (o) For a critical assessment, see, however: Conway, B. E. *Mod. Aspects Electrochem.* **2002**, *35*, 295.

(63) (a) Wang, X. B.; Ding, L. F.; Wang, L. S. *J. Chem. Phys.* **1999**, *110*, 8217. (b) Brink, C.; Andersen, L. H.; Hvelplund, P.; Mather, D.; Volstad, J. D. *Chem. Phys. Lett*. **1995**, *233*, 52. (c) Boltalina, O. V.; Siderov, L. N.; Sukhanova, E. V.; Sorokin, I. D. *Rapid Commun. Mass Spectrom*. **1993**, *7*, 1009.

(64) (a) Dubois, D.; Kadish, K. M.; Flanagan, S.; Robertson, A.; Wilson, L. J. *J. Am. Chem. Soc.* **1991**, *113*, 7773. (b) Dubois, D.; Moninot, G.; Kutner, W.; Jones, M. T.; Kadish, K. M. *J. Phys. Chem*. **1992**, *96*, 7137. (c) Allemand, P.-M.; Koch, A.; Wudl, F.; Rubin, Y.; Diedrich, F.; Alvarez, M. M.; Anz, S. J.; Whetten, R. L. *J. Am. Chem. Soc*. **1991**, *113*, 1050. (d) Yang, Y.; Aries, F.; Echegoyen, L.; Chibante, L. P. F.; Flanagan, S.; Robertson, A.; Wilson, L. J. *J. Am. Chem. Soc.* **1991**, *113*, 7801. (e) Fawcett, W. R.; Opallo, M.; Fedurco, M.; Lee, J. W. *J. Am. Chem. Soc*. **1991**, *113*, 7801. (f) Anderson, M. R.; Dorn, H. C.; Stevenson, S. A. *Carbon* **2000**, *38*, 1663. (g) Carano, M.; Da Ros, T.; Fanti, M.; Kordatos, K.; Marcaccio, M.; Paolucci, F.; Prato, M.; Roffia, S.; Zerbetto, F. *J. Am. Chem. Soc.* **2003**, *125*, 7139.

(65) Zakrzewski, V. G.; Dolgounitcheva, O.; Ortiz, J. V. *J. Phys. Chem.* **1996**, *100*, 16502.

(66) Breslow, R.; Johnson, R. W.; Krebs, A. *Tetrahedron Lett*. **1975**, 3443.

(67) Staley, S. W.; Strand, J. T. *Chem. Phys. Lett.* **1992**, *200*, 527.

(68) Wawzonek, S.; Laitinen, H. A. *J. Am. Chem. Soc*. **1942**, *64*, 2365.

(69) Barinsky, D. J.; Fakuda, E. K.; Campana, J. E. *J. Am. Chem. Soc*. **1984**, *106*, 2770.

(70) Johnson, R. W. *J. Am. Chem. Soc*. **1977**, *99*, 1401.

(71) Green, W. H., Jr.; Gorun, S. M.; Fitzgerald, G.; Fowler, P. W.; Ceulemans, A.; Titeca, B. C. *J. Phys. Chem*. **1996**, *100*, 14892.

(72) For examples of the handling of spin contamination in radicals with different theoretical methods, see: Chuang, Y.-Y.; Coitiño, E. L.; Truhlar, D. G. *J. Phys. Chem. A* **2000**, *104*, 446.